6-2016

CHARACTERIZATION OF INFLUENZA NUCLEOPROTEIN BODY DOMAIN AS ANTIVIRAL TARGET

Alicia Morgan Davis

CHARACTERIZATION OF INFLUENZA NUCLEOPROTEIN BODY DOMAIN AS ANTIVIRAL TARGET

A Thesis

Presented to the

Faculty of

California State University,

San Bernardino

In Partial Fulfillment

of the Requirements for the Degree

Master of Science

in

Biology

---

by

Alicia Morgan Davis

June 2016

CHARACTERIZATION OF INFLUENZA NUCLEOPROTEIN BODY DOMAIN AS ANTIVIRAL TARGET

A Thesis

Presented to the

Faculty of

California State University,

San Bernardino

---

by

Alicia Morgan Davis

June 2016

Approved by:

Laura L. Newcomb, Committee Chair, Biology

Jeremy Dodsworth, Committee Member

Nicole Bournias-Vardiabasis, Committee Member

ABSTRACT

Influenza is a segmented negative strand RNA virus. Each RNA segment is encapsulated by viral nucleoprotein (NP) and bound by the viral RNA dependent RNA polymerase (RdRP) to form viral ribonucleoproteins (vRNPs) responsible for RNA synthesis. NP is a structural component of the vRNP but also interacts with both viral and host factors to regulate viral RNA expression. NP is conserved among influenza A isolates, making NP interactions compelling antiviral targets. Here I characterize mutations within 5 amino acids of NP that comprise an accessible region of the NP body domain, as determined by NP crystal structure. This region was selected for mutagenesis to target interaction between NP and RdRP.

NPbd3 encodes glycine at 5 amino acids within the accessible NP body domain. Cellular fractionation and Western Blot, in addition to NP-GFP fusions and fluorescence, confirm NPbd3 was expressed and localized as WT-NP. Gel shift with purified NP protein confirm NPbd3 bound nucleic acids as WT-NP. Although NPbd3 was expressed, localized, and bound nucleic acid as WT-NP, I found NPbd3 was defective for RNA expression in reconstituted vRNPs, as evaluated by reverse transcription and quantitative polymerase chain reaction (RT-qPCR). To investigate this NP body domain further, single and double amino acid mutations were cloned. Analysis of NP single mutants revealed that all were nearly as functional as WT-NP for RNA expression in reconstituted vRNPs, suggesting these accessible amino acids in the NP body domain play a

redundant role. However, four different combinations of two amino acid mutations resulted in NP double mutants that displayed a significant defect in RNA expression in reconstituted vRNPs, confirming these accessible amino acids in the NP body domain play a significant role for viral RNA synthesis.

A disruption in an essential NP interaction with the RdRP is likely the explanation for the RNA defect observed. In support of this, avian influenza virus passaged in human cells resulted in virus with one NP amino acid change in this domain consistently paired with specific changes in the PB2 subunit of the RdRP. I reason this accessible body domain of NP is a viable antiviral target. Indeed, two amino acids in this NP body domain comprise a novel groove implicated in binding the small molecule inhibitor nucleozin. My thesis highlights this conserved NP body domain as an important interaction surface essential for viral RNA synthesis and support further investigation of antiviral drugs that target this region of NP.

ACKNOWLEDGEMENTS

I would like to thank my tremendous research mentor Laura Newcomb for welcoming me in to her lab, providing this fantastic research project, and encouraging me to pursue a doctorate. I am thankful for Newcomb lab members Jose Ramirez, Alan Santana, Anita Sahagian, Abel Sanchez, and Daniel Smith for contributing time to this project. I would like to thank Dr. Bournias and Dr. Dodsworth for being members of my committee. I would like to thank Dr. Metcalf for allowing me to conduct undergraduate research in his lab. I would like to thank Dr. Sumida for inspiring me to write and publish a review article. I am thankful for the remaining Biology faculty members who helped me become a better scientist through challenging courses and seminar questions. I would like to thank Lisa Anderson for hiring me as a student assistant and continually providing guidance throughout my time at CSUSB. I would like to thank Tom Benson and Dave Coffey for ensuring the Newcomb research equipment was always functional.

I am most grateful for my mother Mary who has been an outstanding role model for me. Her support has been invaluable and directly attributes to my successes today. I would like to thank my father Rick for demonstrating a strong work ethic his entire life. I would also like to thank Brenda, Duane, Cody, Meagan, Sabrina, Jason, and Mike for their unwavering support and love.

TABLE OF CONTENTS

LIST OF TABLES

LIST OF FIGURES

CHAPTER ONE

EMERGING ANTIVIRAL RESISTANT STRAINS OF INFLUENZA A AND THE POTENTIAL THERAPEUTIC TARGETS WITHIN THE VIRAL RIBONUCLEOPROTEIN (VRNP) COMPLEX

Background

This chapter is copied in whole from Davis et al.: Emerging antiviral resistant strains of influenza A and the potential therapeutic targets within the viral ribonucleoprotein (vRNP) complex. Virology Journal 2014 11:167.

Influenza A viruses are infectious agents spread through contact or aerosol droplets that result in a seasonal respiratory illness which can potentially lead to death. Highly transmissible influenza A viruses can reach pandemic proportions as seen in 1918, 1957, 1968, and 2009. The natural reservoir for influenza A viruses are aquatic birds, but many animals are susceptible to infection, including swine and humans. While humans are not readily infected with avian influenza viruses, in rare cases direct avian to human transmission has occurred. Swine are readily susceptible to avian, swine, and human influenza subtypes and provide a vessel for genome reassortment among different subtypes of the virus. The influenza A virus genome is made up of eight negative sense RNA segments (vRNA). Reassortment of genome segments between different influenza A subtypes can yield new influenza A subtypes that have potential to cause a human influenza pandemic. While the 1918 pandemic virus was found to be of wholly avian origin, the 1957 and 1968 pandemics

contained segments of avian and human origin (Reid and Taubengerger, 2003). In this case it is unclear if swine or human were the vessel of reassortment; although swine are more readily infected with avian influenzas, thus providing more opportunity for reassortment, humans can be infected with avian influenza, and although rare, reassortment within a human host remains a possibility (Reid and Taubengerger, 2003). The 2009 influenza H1N1 pandemic contained segments of avian, swine, and human origin and was thus a triple reassortant that likely emerged from swine (Neumann et al., 2009).

Influenza infection is typically prevented by annual vaccination. However, vaccines are not useful after infection or against emerging subtypes of influenza not targeted during vaccine production, as witnessed with the novel H1N1 pandemic in 2009. Therefore, antivirals that target specific proteins to inhibit virus replication are necessary to stave the spread of an emerging pandemic. The eight genome segments of influenza A virus encode 10 different coding mRNAs by way of alternate splicing (Dubois et al., 2014) which result in over 12 proteins due to alternate translation (Chen et al., 2001, Wise et al., 2009, Jagger et al., 2012, Muramoto et al., 2012). Two viral segments code for the surface proteins HA and NA for which influenza subtypes are named. Three viral gene segments encode the RNA dependent RNA polymerase complex: PA, PB1, and PB2. At least two of these genome segments also encode alternate translation products including PB1-F2, PB1-N40, PA-X, PA-N155 and PA-N182 (Chen et al., 2001, Wise et al., 2009, Jagger et al., 2012, Muramoto et al., 2012). One segment

encodes the nucleoprotein NP. Two segments, M and NS, undergo alternate splicing to produce NS1, NS2 (NEP), M1 and M2 proteins. With so many viral protein interactions required in various stages of the influenza life cycle, there are numerous potential target sites for antiviral treatments. Current antivirals target the activities of M2 and NA, but resistance is emerging. This review catalogs the current state of influenza antiviral resistance and describes promising new molecules targeting proteins within the viral ribonucleoprotein (vRNP), the complex comprised of the viral RNA genome, the RNA-dependent RNA polymerase (RdRP), and nucleoprotein (NP).

Current Antivirals and Resistance

The current antivirals approved by the FDA are, in order of their release, Symmetra (amantadine), Flumadine (rimantadine), Relenza (zanamivir), and Tamiflu (oseltamivir). Amantadine and rimantandine are adamantane derivatives that target and inhibit the M2 ion channel. The M2 ion channel is an integral membrane protein responsible for release of vRNPs during infection (Pinto et al., 1992). By binding to the M2 ion channel, amantadine and rimantandine inhibit vRNP release and thus viral replication (Hay et al., 1985, Jing et al., 2008). The antivirals zanamivir and oseltamivir are NA or neuraminidase inhibitors. NA activity is required to release new virions from infected cells (Davis et al., 1983). These drugs inhibit virus release from infected host cells by binding to the active site of the NA protein (Meindl et al., 1974, Palese and Compans, 1974).

Resistance against both classes of influenza antiviral treatments has been

documented. Resistance to M2 ion channel inhibitors occurs via a triple amino acid deletion at residues 28-31 or single amino acid substitutions in the transmembrane region spanning residues 26-31 of the M2 protein (Holsinger et al., 1994, Abed et al., 2005). 100% of H3N2 influenza A viruses circulating in 2009-2010 and 99.8% of 2009 pandemic H1N1 were resistant to adamantanes (CDC-1). Many resistant H1N1 isolates encoded V27A substitution, while resistant H3N2 isolates were found to encode substitutions at L26F, V27A, A30T, S31N, or G34E (Tang et al., 2008). Resistance to adamantanes in H7N9 has also been documented and is acquired by substitution S31N (Chen et al., 2013).

Resistance to NA inhibitors is less common as this class of inhibitors was developed later. For example, 98.9% of tested 2009 H1N1 viruses remained susceptible to oseltamivir, 100% of 2009 H1N1 viruses tested remained susceptible to zanamivir (CDC-2), 100% of influenza A (H3N2) tested remained susceptible to both oseltamivir and zanamivir for the 2012-2013 season (CDC-3). However, multiple single amino acid changes in NA alter susceptibility to the approved neuraminidase inhibitors. Residues V116, I117, E119, Q136, K150, D151, D199, I223, H275, and N295 were selected to monitor for changes that confer drug resistance or reduce efficacy of the antivirals (Deyde et al., 2010). Resistance evolves during treatment, via single amino acid substitutions including changes to amino acids mentioned above such as E119V I223R (Pizzorno et al., 2012, van der Vries et al., 2011), and H275Y (Baz et al., 2009), but also R292K and N294S (Kiso et al., 2004). Pandemic H1N1 2009 isolates

with a substitution at I223R were resistant to neuraminidase inhibitors in addition to M2 ion channel inhibitors as discussed above (van der Vries et al., 2011). Thus, while NA inhibitors are currently still viable to combat most emerging influenza threats, it is only a matter of time before resistance takes hold as with the adamantanes, rendering both current antiviral therapies ineffective against an emerging influenza threat.

Most worrisome is resistance reported among Highly Pathogenic Avian Influenza (HPAI) subtypes that could spur the next pandemic. Avian subtypes such as H5N1, H7N9, and H7N7 have all resulted in human infection. The H5N1 infections result in high morbidity at ~60%, while H7N9 and H7N7 have seen more variability in outcome of human infection (WHO). Fortunately none of these subtypes have gained the ability to transmit readily from human to human, but unfortunately, these strains already have antiviral resistant isolates reported. For example, all H7N9 isolates tested were resistant to adamantanes via the S31N substitution in the M2 protein (Gao et al., 2013), while some H7N9 exhibit high resistance to oseltamivir, mid-resistance to peramivir, and low-resistance to zanamivir via the NA R292K substitution (Hai et al., 2013). Also of grave concern are H5N1 isolates that encode M2 changes to confer resistance to adamantanes and NA changes that reduce susceptibility to neuraminidase inhibitors (Hurt et al., 2007). With many circulating antiviral resistant strains and the consequences of a looming virulent influenza pandemic, novel antiviral targets must be investigated so that new therapies can be developed before such a catastrophic

event occurs. One promising new viral target is the viral ribonucleoprotein or vRNP. Figure 1 depicts vRNP interactions and activities targeted by new anti-influenza candidates.

VRNP: Viral Ribonucleoprotein

During infection eight vRNPs, containing the eight different vRNA genome segments, are released and imported into the nucleus to transcribe and replicate the vRNA. Transcription of the viral genome proceeds via a cellular capped-mRNA primer cleaved from host mRNA by the viral polymerase (Plotch et al., 1981). Unlike other RNA genome viruses, which typically replicate in the cytoplasm, influenza must enter the nucleus to steal nascent host capped mRNAs for use as primers in transcription. The polymerase subunit PA provides the endonuclease activity (Yuan et al., 2009, Dias et al., 2009), while PB2 houses the active site where the host pre-mRNA will bind (33). Polymerization of the viral mRNA transcript proceeds via the PB1 subunit until the polyadenylation signal of repetitive U residues result in stuttering by the viral RdRP and yields the poly(A) tail, terminating transcription (Poon et al., 1999). Transcripts of two influenza genome segments, M and NS, undergo alternative splicing to produce M1, M2, NS1 and NS2 (NEP); utilization of host nuclear splicing machinery is another reason for nuclear localization of influenza vRNPs.

Viral replication occurs *de novo*, without a primer (Shapiro et al., 1988). In the host cell viral RNA replication occurs after translation of viral RdRP and NP proteins. Evidence suggests a model wherein the resident RdRP of the vRNP is

responsible for transcription, while a soluble RdRP is responsible for replication from the vRNA template (Jorba et al., 2009). There are two primer-independent steps of viral replication. First the vRNA template is used to synthesize a full-length complementary (cRNA), which is then replicated to yield progeny vRNA that can be transcribed to mRNA or packaged into new virions during later stages of the viral replication cycle. NP is required for anti-termination at the poly U stretch to allow for replication of full length cRNA (Beaton and Krug, 1986). NP encapsidates both cRNA and vRNA replication products and is necessary for genome length functional cRNPs and vRNPs, respectively (Honda et al., 1988).

NP: Nucleoprotein

The crystal structure of NP (Ye et al., 2006) (Figure 2) reveals two regions termed the body domain and the head domain, between which lies a deep groove comprised of positively charged basic amino acid residues that form ionic bonds with the negatively charged phosphate backbone of viral cRNA and vRNA. On the opposing side of the RNA binding groove lies a tail loop for oligomerization with other NP monomers. The tail loop of NP spans residues 402-428, and is critical to NP oligomerization and RNA binding, as shown through a tail loop deletion mutant that produced primarily monomeric NP unable to oligomerize and bind RNA (Ye et al., 2013). Another crucial oligomerization interaction occurs through a salt bridge between residue 339 of one NP monomer and residue 416 of another NP monomer (Ye et al., 2006, Kao et al., 2009, Shen et al., 2011). Mutational studies disrupting this salt bridge led to

inhibition of viral RNA synthesis *in vitro*, further highlighting the importance of the interaction between NP molecules for vRNP function (Shen et al., 2011).

However, NP is more than a structural RNA binding protein. NP associates with viral proteins such as PB1 and PB2 (Biswas et al., 1998), and M1 (Avalos et al., 1997), in addition to several cellular factors (Portela and Digard, 2002). Interaction between NP and the RdRP enhanced unprimed replication *in vitro*, suggesting the NP-RdRP interaction may regulate the switch from primer initiated transcription to unprimed replication (Newcomb et al., 2009). Interaction of NP with the polymerase subunits was crudely mapped to regions within both the body and head domain of the NP crystal structure (Biswas et al., 1998, Ye et al., 2006). NP-PB2 and NP-PB1 associations were confirmed through co-immunoprecipitation assays in the absence of other viral factors (Biswas et al., 1998). The NP-PB2 interaction was refined to residue 627 and 630 of PB2 and residue 150 of NP, with the strength of NP-PB2 interaction directly correlated with RdRP activity (Ng et al., 2012). Residue R150 of NP is highly conserved and vital for normal viral RNA synthesis during influenza A WSN infection of MDCK cells (Li et al., 2009). As discussed below, PB2 residue 627 is a well-characterized host range determinant (Subbarao et al., 1993, Kuzuhara et al., 2009). Additional NP mutational analysis revealed alanine substitutions within three residues of the head domain at 204, 207, and 208 disrupt interaction with the viral polymerase and inhibit viral RNA synthesis (Marklund et al., 2012). Cryo-EM and cryo-electron tomography data of native vRNPs in packaged

virions revealed two different conformations of polymerase interaction with NP within the vRNP (Arranz et al., 2012). Together, the evidence points to multiple residues on NP that participate in NP-RdRP interactions. The protein sequence homology of NP is a staggering ninety percent among influenza A isolates (Gorman et al., 1990), with the described interaction domains exhibiting even greater homology, highlighting the potential of disrupting NP interactions as an effective antiviral target.

RdRP: RNA Dependent RNA Polymerase

The influenza A virus RNA dependent RNA polymerase is a heterotrimer comprised of PA, PB2, and PB1.

PA. While PA is required for both viral transcription and replication, the major role attributed to PA during influenza infection is the endonuclease activity needed to steal capped primers for viral transcription initiation in the nucleus of a host cell (Plotch et al., 1981, Yuan et al., 2009, Dias et al., 2009, Zhao et al., 2009). Several highly conserved endonuclease active sites span the N-terminal 209 residues of PA (Dias et al., 2009). Alanine screening of amino acids 102 through 134 revealed residues necessary for endonuclease activity (Hara et al., 2006). Substitutions D108A and K134A individually inhibited both endonuclease activity and transcription *in vitro* (Yuan et al., 2009, Hara et al., 2006). PA also makes contacts with both vRNA and cRNA promoters between residues 100-180, though the precise residues involved are debated (Hara et al., 2006, Deng et al., 2006, Maier et al., 2008). In addition, PA has documented protease activity

with Ser 624 defined as the active site (Hara et al., 2006), though the purpose of this activity remains poorly understood. The essential endonuclease activity of PA is an excellent target for antivirals.

PB2. PB2 contains the cap-binding domain, which recognizes the capped structure on nascent host mRNAs to be cleaved by the endonuclease site of PA (Li et al., 2001). PB2 residues 318-483 comprise this domain and contain two aromatic amino acids at positions 363 and 404 necessary for cap-binding (Fetcher et al., 2003, Guilligay et al., 2008). The cap-binding domain of PB2 may also mediate interaction between PB1 and PB2, specifically a loop consisting of residues 421-427 of PB2, which is essential for cap-dependent transcription but not cap-binding, as determined by a deletion mutant (Guiligay et al., 2008). Cap-binding and capped RNA primed transcription are essential activities for influenza that can be targeted by novel antivirals.

PB2 also makes contacts with both vRNA and cRNA promoters in an alpha helix rich region between residues 535-684, which form an RNA binding domain (Kuzuhara et al., 2009). Located within this domain is residue 627, a well-characterized species and pathogenicity determinant for influenza A viruses (Subbarao et al., 1993, Kuzuhara et al., 2009, Massin et al., 2001, Shinya et al., 2004, Labadie et al., 2007, Tarendeau et al., 2008). Avian influenza A viruses encode PB2 with glutamic acid at residue 627, while human influenza A viruses encode lysine (Subbarao et al., 1993). RNA binding ability of PB2 was linked to the amino acid encoded at 627, with increased RNA binding shown for PB2

proteins containing 627K (Kuzuhara et al., 2009). Polymerase activity and interaction of PB2 with NP were also shown to be influenced by PB2 residue 627, in addition to residue 630 (Ng et al., 2012). Characteristic avian PB2 residue E627 must also encode R630 for proper polymerase activity and co-immunoprecipitation with NP (Ng et al., 2012). Characteristic human PB2 residue K627 requires G630 for proper polymerase activity and co-immunoprecipitation with NP (Ng et al., 2012). Residue 627 of PB2 influences binding of NP and RNA, two interactions essential for viral RNA synthesis, making this region of PB2 a favorable target for new antivirals.

PB1. PB1 is the RNA polymerizing subunit of the RNA dependent RNA polymerase. Residues 1-83 and 494-757 of PB1 contribute to vRNA template interaction through *in vitro* analysis of PB1 deletion mutants (González et al., 1999). PB1 interacts with PA through its N terminal domain and PB2 through its C terminal domain, thus forming the functional RNA dependent RNA polymerase (Perez and Donis, 1995, González et al., 1996, Perez et al., 2001, He et al., 2008). RNA dependent RNA polymerase activity of RNA viruses represents a viral activity that can be targeted by antivirals.

The C-terminal domain of PB1 (678-757) and the N-terminal domain of PB2 (1-37) were defined as the regions responsible for PB1-PB2 interaction and were crystalized to facilitate further investigation (González et al., 1996, Sugiyama et al., 2009). Crystal structure of this interaction reveals all contacts occur through helix 1 of PB2 (residues 1-12), which is essential for proper RNA

polymerase activity (Sugiyama et al., 2009). The PB1-PB2 protein interface is of great interest as an antiviral target due to the conservation of these domains in both human and avian viruses (Sugiyama et al., 2009).

The N-terminus of PB1 (1-80) interacts with the C terminal region of PA consisting of residues 239-716 (González et al., 1996, Krug and Aramini, 2009). Interaction surfaces of both PB1 and PA are highly conserved (He et al., 2008, Wunderlich et al., 2009, Obayashi et al., 2008). The crystal structure of this interaction reveals PB1 N terminal 25 residues occupy a C-terminal hydrophobic groove of PA (68) (Figure 3). The C-terminal domain of PA has been referred to as a “dragon’s head” that holds the N-terminus of PB1 in its “jaws” (He et al., 2008). A peptide analog of the N-terminal 25 amino acids of PB1 blocks formation of the RNA dependent RNA polymerase complex resulting in no viral replication (He et al., 2008, Ghanem et al., 2007). These studies demonstrate the critical interaction between PB1 and PA in the formation of the RNA dependent RNA polymerase heterotrimer vital for viral RNA synthesis, making this interaction a potential target for novel antivirals.

New Antivirals Targeting Influenza A VRNP

The critical roles of the influenza vRNP for viral RNA synthesis make activities of the vRNP, such as cap-snatching and RNA polymerization, excellent antiviral targets. A recently discovered nucleotide analog preferentially utilized by viral RNA dependent RNA polymerases including influenza vRNP, is under study as a promising antiviral therapy targeting the activity of viral RNA dependent

RNA polymerases (Furuta et al., 2002). Further, the multiple essential interactions of the vRNP, such as with each other to form the RNA dependent RNA polymerase heterodimer, with host capped mRNAs to obtain primers for viral transcription, and with NP to regulate and enhance RNA replication, coupled with high conservation of these domains among influenza subtypes, make the proteins of the vRNP excellent targets for small molecule inhibitors with broad efficacy against multiple influenza A subtypes.

Ribonucleotide Analogs

Favipiravir is a 6-fluoro-3-hydroxy-2-pyrazinecarboxamide molecule (also known as T-705) that upon phosphorylation becomes favipiravir-ribofuranosyl-5'-triphosphate (RTP) and inhibits many viral RNA dependent RNA polymerases (75). Favipiravir is effective against influenza A, influenza B, influenza C, hantaviruses, flaviviruses, noroviruses, and most recently ebola viruses (Furuta et al., 2002, Furuta et al., 2013, Oestereich et al., 2014). The T-705 RTP is erroneously interpreted as a purine nucleotide by the viral polymerase during RNA elongation (Furuta et al., 2013, Jin et al., 2013). Once incorporated into the elongating viral RNA, the analog may hinder strand extension (Jin et al., 2013). The antiviral activity of Favipiravir includes influenza A(H3N2), A(H1N1), A(H5N1), A(H7N9), and strains bearing resistance to both classes of the current FDA approved influenza antivirals (Furuta et al., 2002, Furuta et al., 2013, Sleeman et al., 2010).

The 50% inhibitory concentration (IC_{50}) of favipiravir for influenza, determined by plaque reduction assay, was 0.013-0.48 μg/ml with no cytotoxic effect up to 1000 μg/ml (Furuta et al., 2002). Human DNA polymerase α, β, or γ with 1000 μM of favipiravir showed little sign of inhibition (Kiso et al., 2010) and human RNA polymerase II had an IC_{50} of 905 μM of favipiravir (Takahashi et al., 2011). Therefore, the IC_{50} of host polymerases is well over 2000 times greater then the IC_{50} for influenza vRNP, making favipiravir highly selective for influenza vRNP (Furuta et al., 2013). Favipiravir for influenza therapy has finished two Phase II clinical trials in the United States and one Phase II clinical trial in Japan (Furuta et al., 2013). Favipiravir is a favorable candidate for a broadly effective antiviral therapy targeting RNA viruses with RNA dependent RNA polymerases that preferentially incorporate favipiravir in RNA synthesis. It is not yet clear if or how quickly influenza vRNP will evolve resistance to this nucleotide analog, but based on HBV and approved nucleotide analog therapies (Menéndez-Arias et al., 2014), as with any antiviral therapy, if resistance is possible, it will eventually develop, stressing the need to consistently look for novel antiviral targets and therapies.

Small Molecule Inhibitors

Unlike nucleotide analog therapies, small molecule inhibitors work by interaction with a viral protein to block a function or interaction and inhibit viral replication. Crystal structure data provides much information to identify small molecules with potential to bind a domain of the target protein and inhibit

essential functions or interactions. Small molecules that target conserved regions are likely to have the best efficacy against multiple subtypes. Further, conserved regions are less likely to tolerate mutation and evolve a viable virus with resistance to the small molecule.

Targeting NP

Nucleozin is a small molecule inhibitor of NP that works by promoting NP oligomerization, blocking nuclear entry through aggregation of NP molecules at the nuclear membrane (Kao et al., 2010) and inducing vRNP aggregation during cytoplasmic trafficking (Amorim et al., 2013). Molecular docking models identified two proposed nucleozin interaction sites at residue 289 and 309 of NP (Kao et al., 2010). Both residues participate to stabilize the interaction; a tyrosine at residue 289 forms aromatic ring stacking with nucleozin, while an asparagine at residue 309 shares a hydrogen bond with nucleozin. Strains found to be nucleozin resistant encoded a histidine in place of a tyrosine at residue 289 of NP (Kao et al., 2010). From the crystal structure of NP, residue 289 is relatively accessible to interact with nucleozin (Figure 2) (39, Kao et al., 2010). The 289H NP variant likely disrupts a critical point of interaction between NP and nucleozin. Sequence analysis of the NP gene of 3,881 influenza strains revealed Y289H substitution in 527 strains. Unfortunately the A(H1N1)pdm09 strain was shown to contain this single amino acid alteration, signifying it as a nucleozin resistant strain (Kao et al., 2010). Nucleozin demonstrated a 50% effective concentration (EC_{50}) of only 0.069 μM against influenza with 50% cytotoxic concentration

greater than 250 μM (Kao et al., 2010). Thus nucleozin still holds potential as a potent antiviral for strains of influenza housing a tyrosine at residue 289 (Kao et al., 2010). In addition to nucleozin, there are several other aryl piperazine amide compounds discovered in parallel that target NP and inhibit virus replication in the same manner (Kao et al., 2010, Su et al., 2010, Gerritz et al., 2011, Cianci et al., 2013). Cianci et al. provide a detailed review into the efficacy of aryl piperazine amides, including nucleozin, as NP inhibitors (Cianci et al., 2013). Further analysis of these compounds could lead to the synthesis of an optimized aryl piperazine amide inhibitor of viral replication, even against the circulating nucleozin resistant strains of influenza.

The essential salt bridge for NP oligomerization at residues 339 and 416 was targeted for disruption by small molecule inhibitors (Figure 2) (Shen et al., 2011). Peptides that mimicked the NP tail loop (residues 402-428) bound in the tail loop binding pocket and inhibited NP oligomerization, resulting in decreased viral replication by greater than fifty percent (Shen et al., 2011). Random virtual screening of small molecules identified four compounds (termed # 3, 7, 12, and 23) that interrupt NP oligomerization and decrease viral replication (Shen et al., 2011). The IC_{50} of compounds 3, 7, 12, and 23 ranged from 2.4 to 118 μM in cells challenged with influenza A/WSN/33 for nine hours at a multiplicity of infection (MOI) of 0.2 (Shen et al., 2011). Although the targeted NP domain is highly conserved, more research will need to be carried out to ensure little to no development of resistance to the compounds. Importantly, cytotoxicity of these

compounds will need to be assessed before they can be of use as antiviral therapies.

Mycalamide A is an antiviral and antitumor compound isolated from *Mycale* sponges but is unfortunately toxic to cells (Perry et al., 1988). A photo-cross-linked chemical array identified analogs of mycalamide A that possess the ability to bind NP (Hagiwara et al., 2010). One compound inhibited viral replication up to 77% in a plaque assay using influenza virus (A/WSN/33) with no cytotoxic effect (Hagiwara et al., 2010). Binding affinity of the analogs was greatest within the N-terminal 110 amino acids of NP (Hagiwara et al., 2010). Although the mechanism of inhibition remains uncharacterized, the N-terminus of NP contains an important non-canonical nuclear localization signal (NLS) (Wang et al., 1997, Cros et al., 2005) and interacts with host RNA processing factors UAP56 and URH49 (Momose et al., 2001, Wisskirchen et al., 2011) proposed to enhance RNA replication (Kawaguchi et al., 2011). More research is needed on these compounds to elucidate the mechanism of inhibition and determine if or how quickly influenza NP will evolve resistance.

Naproxen is an over the counter nonsteroidal anti-inflammatory drug that inhibits NP from associating with RNA in the RNA binding groove (Figure 2) (Lejal et al., 2013). From several molecular docking studies, residues Y148, Q149, R150, R355, R361, and F489 are believed to stabilize naproxen binding to NP (Lejal et al., 2013). Naproxen acts selectively upon monomeric NP and was shown to protect MDCK cells and mice from a viral challenge at an MOI of 10^{-2} -

10^{-3} or 50 - 2,000 PFU respectively, with little to no cytotoxic effects (Lejal et al., 2013). Subtypes of H1N1 and H3N2 were both susceptible to inhibition and treatment resulted in efficient protection from viral challenge with either subtype (Lejal et al., 2013). No escape mutant viruses were produced in response to 500 μM naproxen treatment in cells after six passages (Lejal et al., 2013). Within this experiment the mode of delivery for naproxen was intraperitoneal injection or intranasal treatment in mice that displayed an EC_{50} of 40mg/kg (Lejal et al., 2013). Naproxen is currently used as an oral medication with a recommended dosage of 220 mg every 8 hours for pain. Naproxen is not currently used as an antiviral but could be optimized for antiviral use through further experimentation and improved drug design.

Targeting PA-PB1 Interaction

Inhibitors of the PA-PB1 interaction are numerous (Muratore et al., 2012). Compound 1 was discovered through *in silico* screening (Muratore et al., 2012) using the crystal structure of PA_C-$PB1_N$ (Figure 3) (He et al., 2008). The hydrophobic pocket of PA houses compound 1 according to molecular docking studies, and inhibition of PA-PB1 interaction was demonstrated through ELISA and immunoprecipitation of PA (Muratore et al., 2012). Compound 1 inhibited RNA polymerase activity in a dose-dependent manner with an IC_{50} of about 18 μM assessed in a minireplicon assay using a firefly luciferase reporter gene, with no significant cytotoxic effect up to concentrations of 250-1000 μM (Muratore et al., 2012). Compound 1 inhibited viral replication in MDCK cells for several

influenza A H1N1 and H3N2 strains, a swine-origin influenza virus, and an oseltamivir-resistant isolate, with IC_{50} ranging from 12.2 to 22.5 μM (Muratore et al., 2012).

There are two FDA approved medications that in addition to their intended use also possess anti-IAV abilities due to their structural similarity with the N terminal domain of PB1 that interacts with the C-terminus of PA (Figure 3) (Fukuoka et al., 2012). Benzbromarone is approved to treat gout and hyperuricemia by promoting the excretion of uric acid. Diclazuril is most commonly used in veterinary medicine as an anti-coccidial. Although these drugs are FDA approved, appropriate drug dosages for use against viral challenges would need to be established before they could be employed for use against influenza A. Testing for the ability of viruses to gain resistance to these drugs must also be done. Benzbromarone and diclazuril could potentially be utilized if an influenza strain arises that possesses resistance to other antivirals available (Fukuoka et al., 2012).

In addition, a compound derived from licorice, 18β-glycyrrhetinic acid (GHA), is a naturally occurring compound that exhibits some anti-IAV activity attributed to interaction with the C terminal domain of PA (Li et al., 2012). Molecular docking studies identified GHA as a ligand to PA_C (Li et al., 2012). GHA decreased polymerase activity 80%, as assessed by a primer extension assay for cRNA synthesis (Li et al., 2012). These preliminary findings need to be investigated further with more informative assays including *in vitro* PA-PB1

interaction inhibition study, *in vivo* polymerase activity assays in tissue culture, and *in vivo* infection in an animal model. There are many small molecules that mimic the N terminus of PB1 fit in the hydrophobic groove of PA to inhibit PA-PB1 interaction (Figure 3) and should be studied further for their potential as an anti-influenza A treatment.

Targeting PA Endonuclease

Fullerene (C_{60}) is a spherical molecule of sixty carbon atoms that exhibits anti-influenza activity (Shoji et al., 2013). Full length PA and an isolated PA endonuclease domain were tested in an *in vitro* endonuclease assay in the presence of fullerene derivatives. Seven fullerene derivatives were able to inhibit the endonuclease ability of the full length PA and isolated endonuclease domain (Shoji et al., 2013). Docking simulations reveal the fullerene skeleton fits nicely into the endonuclease domain active pocket (Shoji et al., 2013). MDCK cells were infected with influenza A H1N1 or H3N2 mixed with 0 to 100 μM fullerene derivative and immunostained for NP at 24 hours post infection to reveal significantly less NP in cells infected with virus pre-incubated with fullerene compared to a DMSO control (Shoji et al., 2013). Twelve derivatives of fullerene were tested and resulted in varying efficacy against influenza but showed no cytotoxic effect up to 100 μM (Shoji et al., 2013). More investigation into the activity and expression of viral proteins in response to fullerene needs to be conducted. Importantly, treatment applied post-infection needs to be

investigated. This novel compound exemplifies yet another possible antiviral target within the vRNP.

Targeting PB2 Cap-binding Domain

Compounds that mimic the 7-methylguanosine moiety of the 5' cap of mRNAs may serve as transcriptional inhibitors. Docking studies of the cap-binding domain of PB2 revealed 7-alkylguanine derivatives as potential inhibitory compounds (Pautus et al., 2013). Several compounds bind the cap-binding domain of PB2 with greater affinity than a biotinylated cap analogue (Pautus et al., 2013). These compounds should be further studied and optimized for anti-influenza activity.

Conclusion

Influenza A virus continues to remain a human menace, in terms of both human health and global economic costs. The wide host range of influenza A virus, coupled with a lack of proofreading activity within the viral RNA dependent RNA polymerases, and a segmented RNA genome allowing for segment reassortment, provide influenza A virus with the ability to evolve rapidly. While yearly vaccination is protective against the strains and subtypes predicted to be circulating and represented during vaccine production, vaccination will not protect against an unseen, emerging subtype of the virus. Antivirals are the first line of defense for an emerging pandemic and resistance to current antivirals is already circulating within influenza A viruses, hastening the resolve to identify new antiviral therapies. The viral ribonucleoprotein (vRNP) is essential for viral

replication, making it an ideal target for antivirals. Essential activities of the vRNP include cap-snatching activity required for viral mRNA transcription and RNA polymerase activity required for viral mRNA transcription and RNA replication. The interactions required to form functional vRNPs with these essential activities comprise the most highly conserved protein domains within influenza A subtypes. These interaction domains represent ideal targets for small molecule inhibitors, as these domains are less likely to tolerate mutations. Combination drug therapy is also a potential means to challenge emerging antiviral resistance. The vRNP provides multiple viral protein targets to reduce selection pressures and emergence of resistant strains. However, if mutations conferring antiviral resistance are tolerated, history dictates these mutations will be selected by use of the antiviral and propagate in circulating influenza A viruses. This means the search for new influenza A antiviral inhibitors should be ongoing until a universal vaccine is achieved.

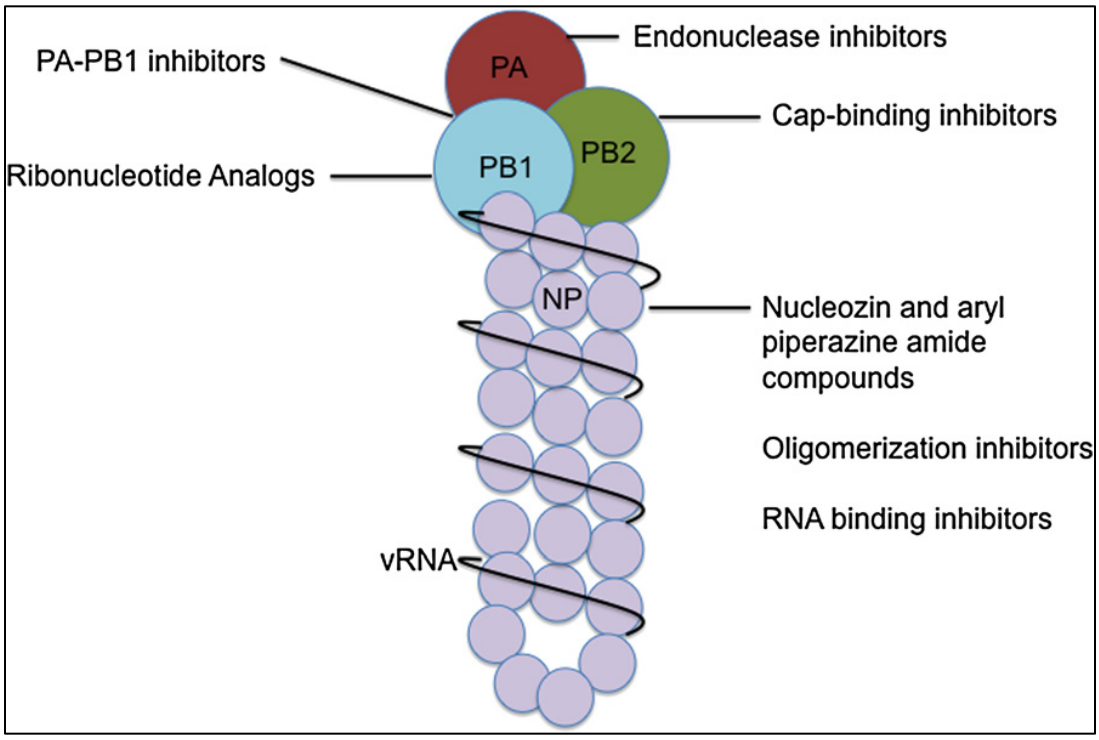

Figure 1. Antiviral Targets of Viral Ribonucleoprotein.

Anti-influenza candidates include small molecule inhibitors that disrupt critical functions or interactions within the vRNP. This figure provides a summary of the promising anti-influenza candidates discussed in this review. Davis et al.: Emerging antiviral resistant strains of influenza A and the potential therapeutic targets within the viral ribonucleoprotein (vRNP) complex. Virology Journal 2014 11:167.

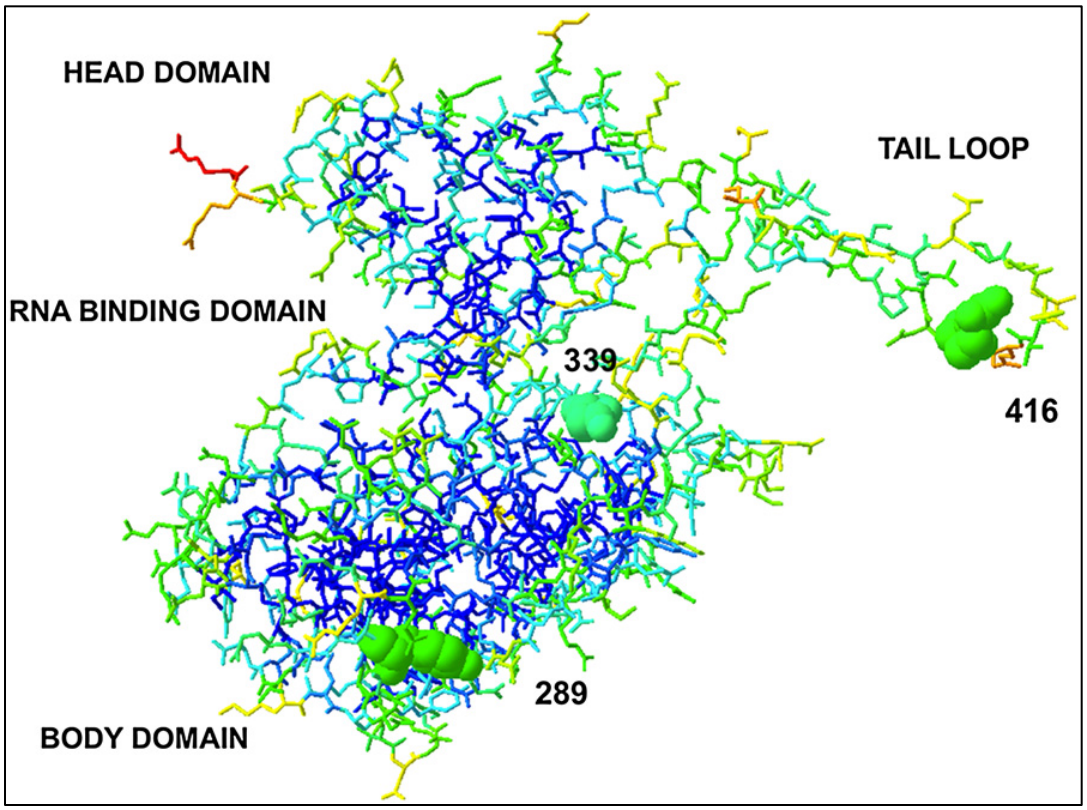

Figure 2. Antiviral Targets of Nucleoprotein.

Analysis of NP monomer crystal structure extracted from NP trimer crystal structure “2IQH” (Ye et al., 2006) using Deep View-Swiss-PdbViewer 4.0. Residue color determined by accessibility. Greatest to least accessible as follows: red, orange, yellow, green, light blue, and dark blue. Residue 289 is the proposed site of interaction with the antiviral compound nucleozin (Kao et al., 2010). An intermolecular salt bridge formed by residues 339 and 416 of NP is essential for oligomerization and can be disrupted by small molecule inhibitors (Shen et al., 2011). Davis et al.: Emerging antiviral resistant strains of influenza A and the potential therapeutic targets within the viral ribonucleoprotein (vRNP) complex. Virology Journal 2014 11:167.

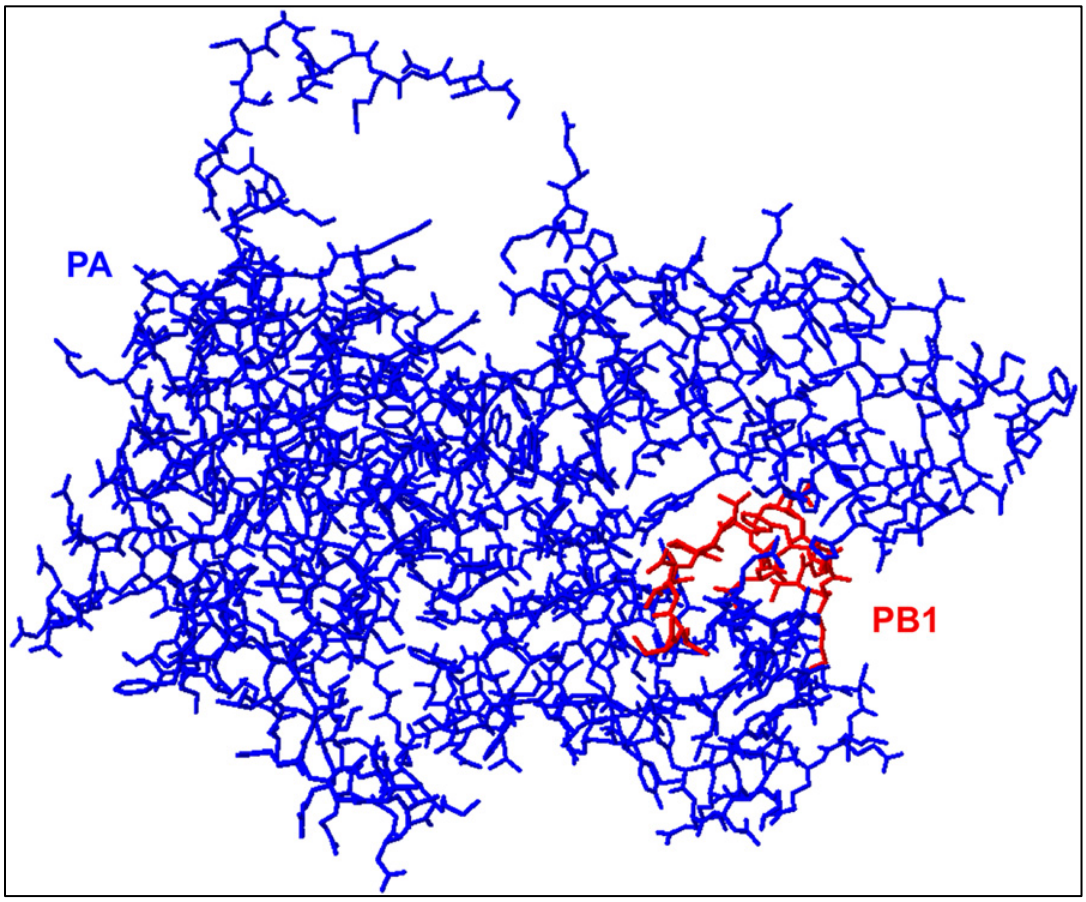

Figure 3. PA-PB1 Interaction Site is an Antiviral Target.

Analysis of the PAC-PB1N crystal structure “3CM8” (He et al., 2008) using Deep View-Swiss-PdbViewer 4.0. Residues 1–16 of PB1 (red) are shown in interaction with residues 258–716 of PA (blue). Many small molecule inhibitors of PA resemble the N terminus of PB1 and bind in the hydrophobic pocket blocking essential interactions between the polymerase subunits (He et al., 2008, Ghanem et al., 2007, Fukuoka et al., 2012). Davis et al.: Emerging antiviral resistant strains of influenza A and the potential therapeutic targets within the viral ribonucleoprotein (vRNP) complex. Virology Journal 2014 11:167.

CHAPTER TWO

MUTATIONAL ANALYSIS OF NUCLEOPROTEIN DOMAINS

Identification and Development of Nucleoprotein Mutants

Previous work in our lab investigated potential antiviral targets within NP by carefully analyzing the protein crystal structure (Ye et al., 2006) to identify accessible regions. The RNA binding pocket, head domain, and body domain (Fig. 4) were examined by amino acid substitutions created through cloning. The RNA binding pocket mutant, NPrbp1, encoded R152A while the head domain mutant, NPhd1 was altered at amino acids R213A and K214A. Five regions of the NP body domain were investigated through the following mutants: NPbd1 (E46A, K48A), NPbd2 (D101A), NPbd3 (Y289G, K293G, E294G, Q308G, N309G), NPbd4 (S482A), and NPbd5 (S467G, E469G, N470G, T471G, and N472G).

Viral Ribonucleoprotein Activity

Activity of each NP mutant was tested using the reconstituted viral ribonucleoprotein (vRNP) expression system (Fig. 5). Plasmids to express mRNA encoding PB1, PB2, PA, and either NP, no NP, or NP mutant, were transfected into 293T cells along with plasmid to express Green Fluorescent Protein (GFP) M vRNA, the negative sense vRNA segment of the reconstituted vRNP. GFP positive cells within this system represent viral gene expression. GFP expression was observed 48 hours post transfection. All NP mutants expressed GFP at

similar levels as wild type NP (WT-NP) except NPbd3, the third of five body domains mutants constructed (Table 1 and Fig. 6). NPbd3 was investigated further for this master's thesis.

I next examined the activity of reconstituted vRNPs comprised of NPbd3 at the level of RNA. The defect in viral protein expression observed with NPbd3 is reflected at the RNA level. To directly examine both viral plus sense RNA synthesis (c/mRNA) and the second step in replication, negative sense RNA synthesis (vRNA), the reconstituted expression system was carried out with either an influenza M cRNA or M vRNA template. RNA was isolated from cells, DNAse treated, reverse transcribed with oligo dT (vRNA template) or vRNA specific primer (cRNA template), and subjected to qPCR analysis targeting the M gene. NPbd3 was found to be defective for viral c/mRNA synthesis as compared to WT-NP (Fig. 7) and vRNA synthesis when compared to the relative expression of WT-NP (Fig. 7).

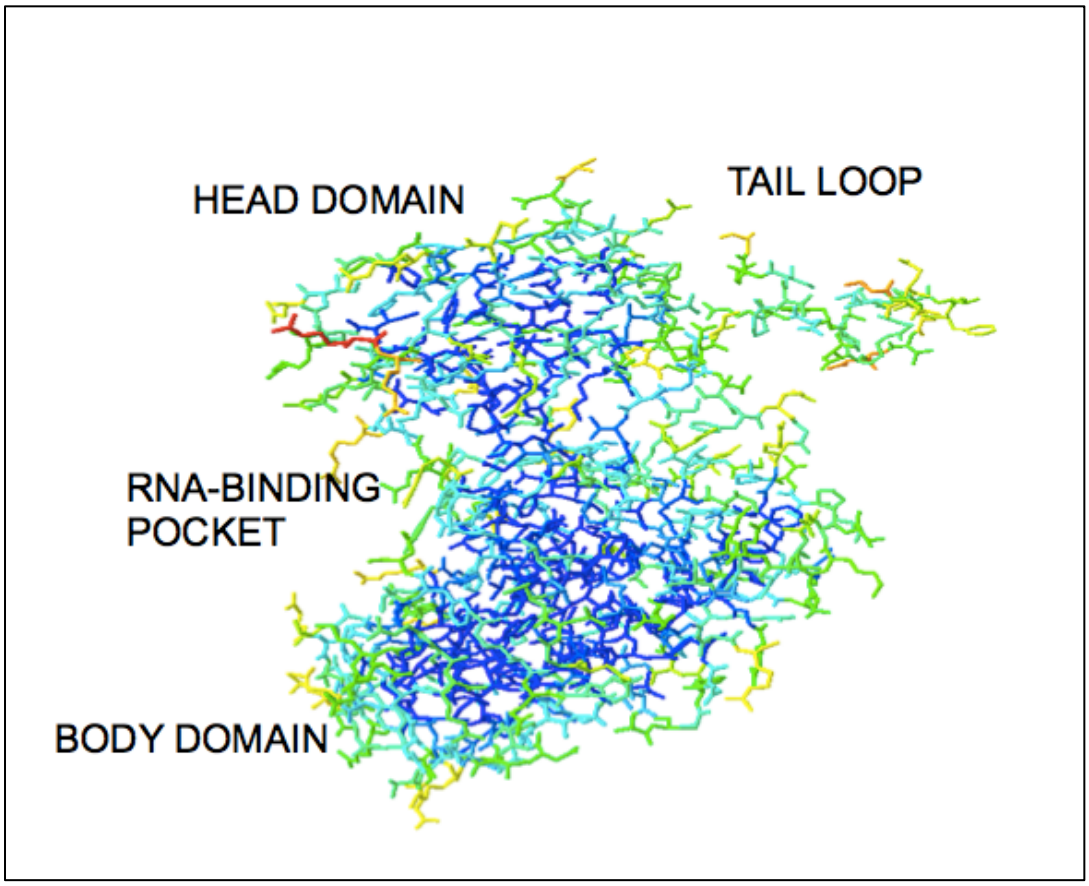

Figure 4. Domains of NP.

Analysis of NP monomer crystal structure (Ye et al., 2006) colored by accessibility using Deep View-Swiss-PdbViewer 4.0. Greatest to least accessible as follows: red, orange, yellow, green, light blue, and dark blue.

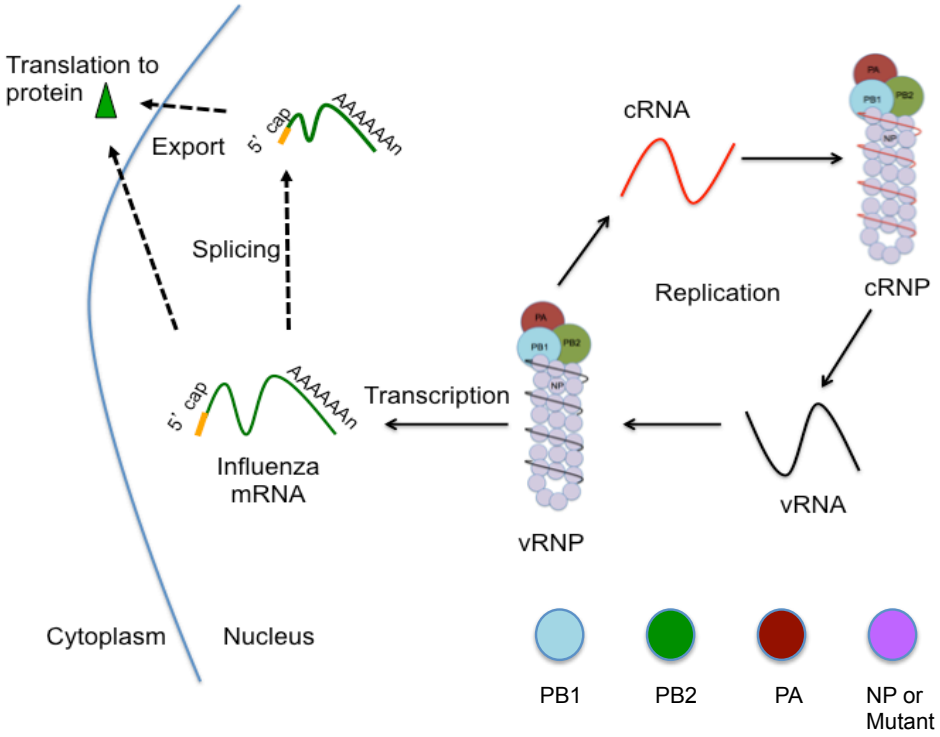

Figure 5. Reconstituted Ribonucleoprotein Expression System.

pcDNA expression vectors of PB1, PB2, PA, and NP or mutant are transfected into 293T cells to express RNPs. A pHH21 expression vector containing a genomic cRNA or vRNA template is also transfected. Cellular RNA polymerase I drives expression of the cRNA or vRNA template from pHH21. Cellular RNA polymerase II drives expression of viral mRNAs from pcDNA3 encoding plasmids.

Table 1. NP Mutant Analysis.

NP Mutant	NP Domain	NP amino acid changes	Functional vRNP - GFP as reporter
NPrbp1	RNA binding pocket	R152A	YES
NPbd1	Body domain	E46A, K48A	YES
NPbd2	Body domain	D101A	YES
NPbd3	Body domain	Y289G, K293G, E294G, Q308G, N309G	NO
NPbd4	Body domain	S482A	YES
NPbd5	Body domain	S467G, E469G, N470G, T471G, N472G	YES
NPhd1	Head domain	R213A, K214A	YES

Seven NP mutants in regions of the RNA binding pocket, body domain, or head domain were constructed and tested for GFP activity in the reconstituted RNP expression system. (Laura Newcomb)

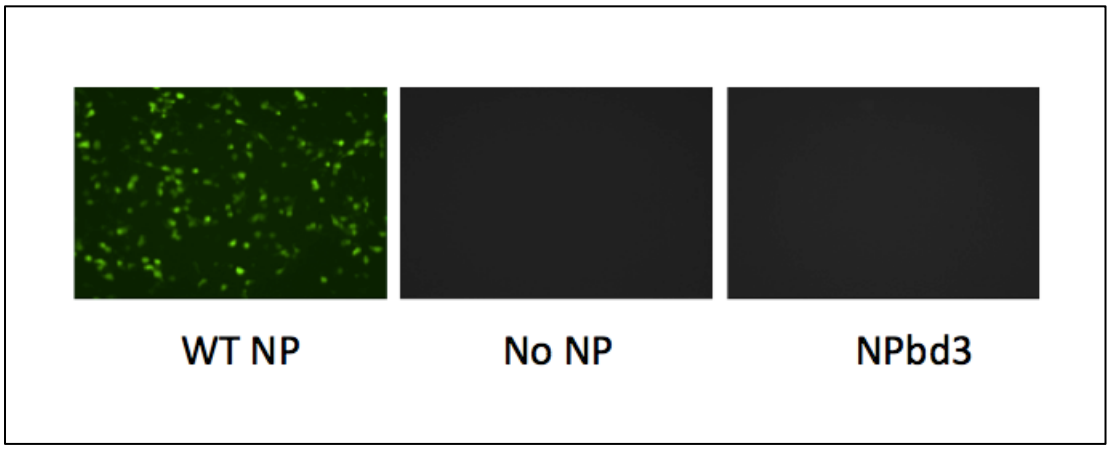

Figure 6. NPbd3 is Defective for Viral Protein Expression.

Plasmids to express reconstituted vRNPs with GFP-M vRNA and either WT-NP, no NP, or NPbd3 were transfected into 293T cells. 48 hours post transfection cells were observed for GFP-M expression. WT-NP represents the positive control while no NP is the negative control. GFP was visualized with a Nikon Eclipse TS100 (Nikon Intensilight C-HGFI for fluorescence) inverted microscope and images captured with the Nikon DS-Qi1Mc camera with NS Elements software.

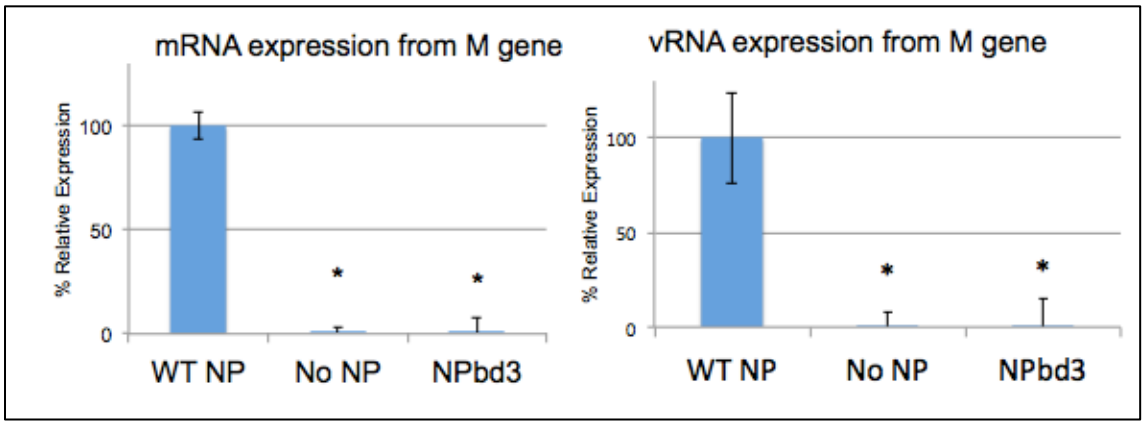

Figure 7. NPbd3 is Defective for Viral RNA Expression.

RNA was purified from cells expressing reconstituted vRNPs or cRNPs as indicated. 1 µg was DNase treated and subject to reverse transcription with oligo dT and quantitative PCR with gene specific primers to calculate relative M RNA expression in each sample. Data are from triplicate trials; asterisks indicate $p<0.02$.

CHAPTER THREE

CHARACTERIZATION OF NUCLEOPROTEIN BODY DOMAIN MUTANT #3

Background

The amino acid substitutions in NPbd3 were selected for mutagenesis to target interaction between NP and RdRP (Biswas et. al., 1998). The amino acids chosen were based on relative sequence conservation (Fig. 8) and accessibility in regards to the surface of the protein (Fig. 9) determined by examining the cryo-electron microscopy (cryo-EM) structure of mini-vRNPs (Coloma et. al., 2009) and NP crystal structure (Ye et. al., 2006). Of seven NP mutants constructed, NPbd3 was the only mutant to be completely defective for protein expression in a reconstituted vRNP assay and was also found to be defective in viral RNA synthesis. These results highlighted the importance of the substituted amino acids and led to the characterization of NPbd3.

Viral Ribonucleoprotein Activity

Expression and Localization

To ensure NPbd3 was expressed and localized as WT-NP cellular fractionation and Western blot were performed. Cells were collected and fractionated using non-ionic detergent and centrifugation as in materials and methods. Cellular fractions were analyzed by Western blot using anti-FLAG and anti-Hsp90 antibodies. NPbd3 is expressed and localized as WT-NP (Fig. 10). To further confirm localization of NPbd3, NP-GFP and NPbd3-GFP fusion proteins

were constructed and observed through fluorescence microscopy. Again NPbd3 was localized in a pattern similar to WT-NP 48 hours post transfection (Fig. 11).

NPbd3 was expressed at a slightly lower level than WT-NP in many of our location experiments (Fig. 10). To verify that NP is expressed in excess in the reconstituted vRNP assay and confirm decreased expression of NPbd3 was not responsible for the defect observed, we titrated WT-NP expressing plasmid in transfection from 600 nanograms to 100 nanograms. As expected, lowering plasmid amount during transfection did result in decreased NP protein expression (Fig. 12). Titration activity was examined in the reconstituted expression system using a GFP MvRNA template and confirms that even transfection of 100ng DNA plasmid resulted in little change in GFP expression (Fig. 13). While 100ng of NP expression plasmid and 600ng NPbd3 expression plasmid result in similar NP protein expression (Fig.12), they do not have similar vRNP activity as represented by GFP expression (Fig. 13). These experiments confirm NP is in excess in our standard reconstituted vRNP assay and that the lower NPbd3 expression is not the cause of the lack of activity.

RNA Binding and Oligomerization

NP binds viral RNA and through oligomerization provides the basic structure for the vRNP. There is one NP monomer for approximately 24 nucleotides of RNA (Ye et. al., 2006). To confirm NPbd3 did not result in a defect in RNA binding, we performed an electrophoretic mobility shift assay (EMSA). WT-NP and NPbd3 were immunopurified with FLAG antibody coupled to agarose

beads. Immunopurified NP proteins were analyzed by SDS-PAGE and Coomassie Blue stain to ensure no additional protein contaminants (Fig. 14). Incubation of purified proteins with biotin labeled single stranded nucleic acid followed by non-denaturing Native PAGE and Western blot with HRP-Streptavidin confirmed NPbd3 bound nucleic acids as WT-NP (Fig. 14A). The Coomassie Blue stain shows a great deal of purified WT-NP but very little NPbd3 (Fig. 14B), which is reflected in the amount of nucleic acid bound. Although there is a difference in the expression and concentration of protein, we can conclude NPbd3 binds nucleic acid. Additionally, a preliminary gel shift demonstrated equal amounts of WT-NP and NPbd3 binding nucleic acid but contained a great deal of background. NP oligomerization is important for RNA binding and formation of functional vRNPs. To examine NP oligomer formation, protein extracts from cells expressing WT-NP or NPbd3 were separated by blue native polyacrylamide gel electrophoresis (BN-PAGE) followed by western blot with anti-FLAG antibody. Results demonstrate the ability of WT-NP and NPbd3 to form oligomers (Fig. 15).

Although NPbd3 was expressed in the cell, localized as WT-NP, found in oligomers, and bound nucleic acid *in vitro*, NPbd3 was defective for viral RNA expression in reconstituted vRNPs and cRNPs. I next decided to further define the important residues within this domain of NP.

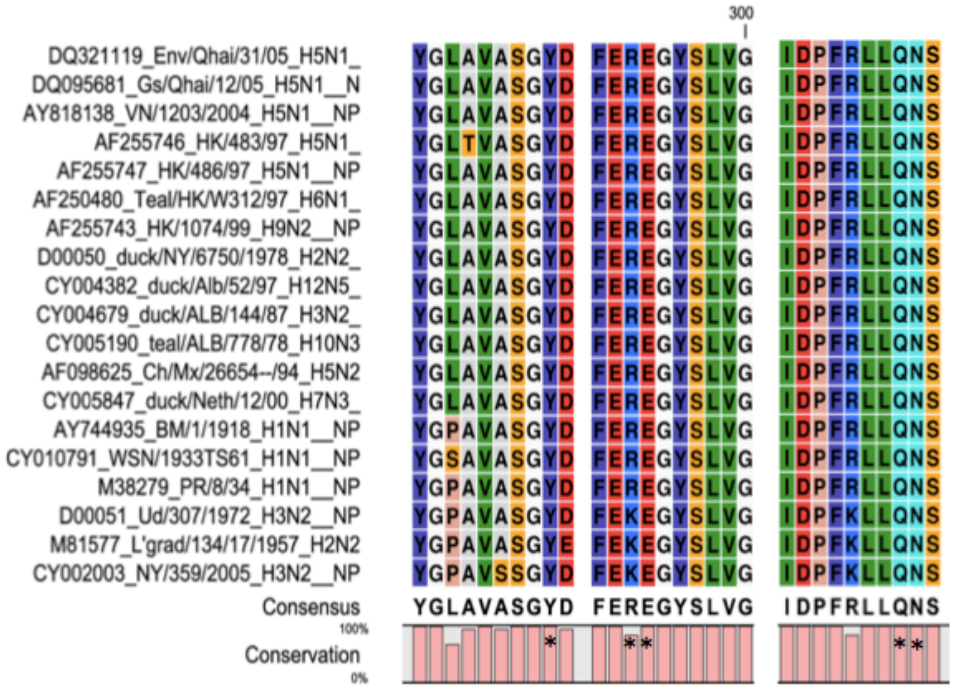

Figure 8. Sequence Alignment of NPbd3 Residues.

Percent conservation and consensus amino acids of NPbd3 are denoted with asterisks. Amino acid 289, 293, 294, 308, and 309 are highly conserved in the influenza strains utilized in the sequence alignment. (Laura Newcomb).

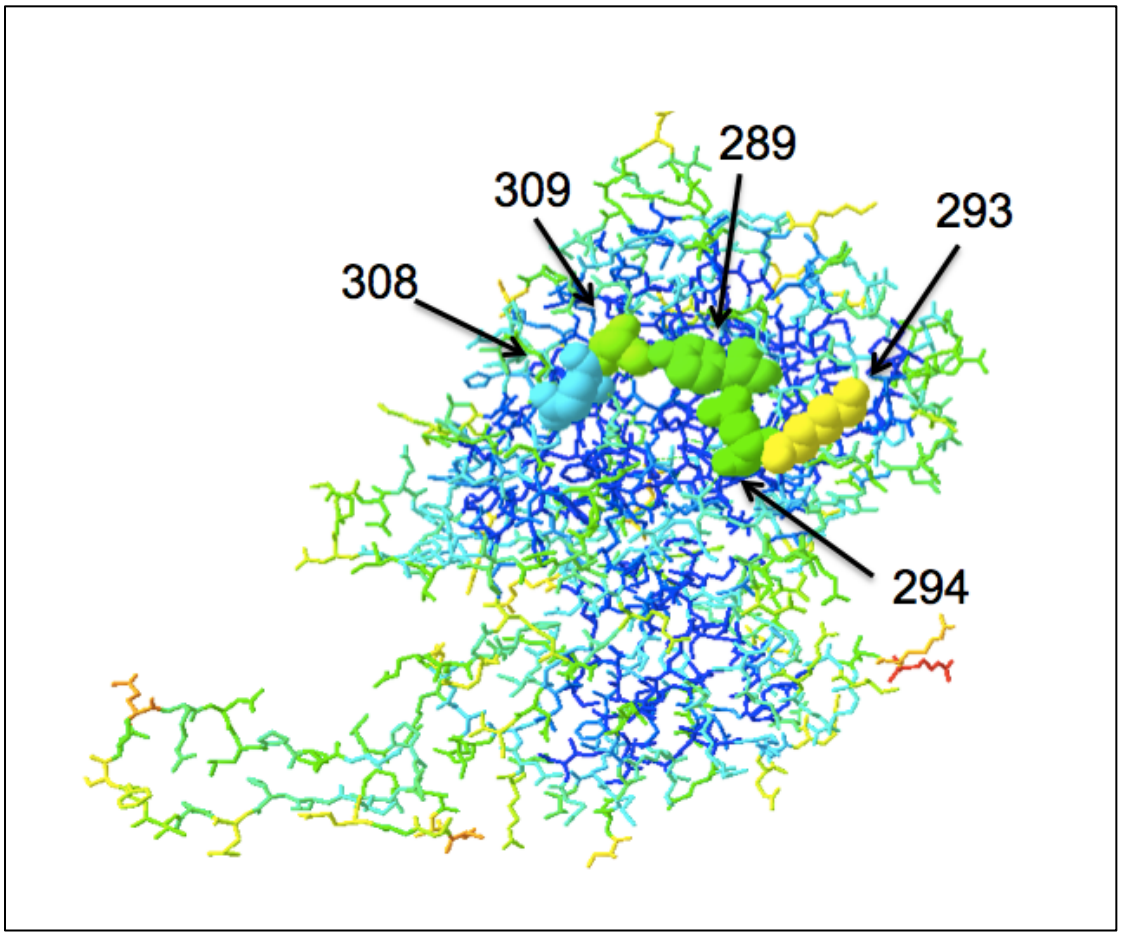

Figure 9. NP Body Domain Substitutions of NPbd3.

Deep View-Swiss-PdbViewer 4.0 was used to analyze accessible residues in the body domain of the NP monomer crystal structure (Ye et al., 2006). Residues 289, 293, 294, 308, and 309 were mutated in NPbd3 and are highlighted here. Residue color determined by accessibility. Greatest to least accessible as follows: red, orange, yellow, green, light blue, and dark blue.

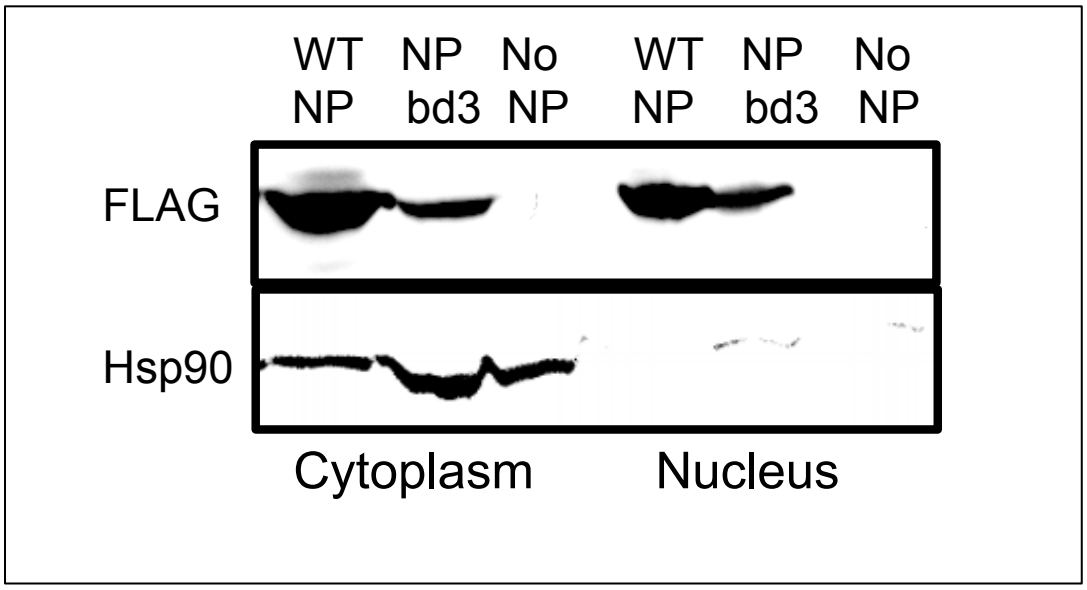

Figure 10. NPbd3 is Expressed and Localized as WT-NP.

Cells expressing reconstituted vRNPs were collected and fractionated with NP-40 non-ionic detergent to break open cellular plasma membrane. Microscopy was used to confirm disrupted plasma membranes and intact nuclei. Nuclei were pelleted by centrifugation and proteins isolated. Proteins were separated on a 10% SDS PAGE and transferred to nitrocellulose. Western blot was performed with anti-FLAG to detect WT-NP and NPbd3 and anti-Hsp90 to detect Hsp90, a protein localized in the cytoplasm, which serves as confirmation of cellular fractionation.

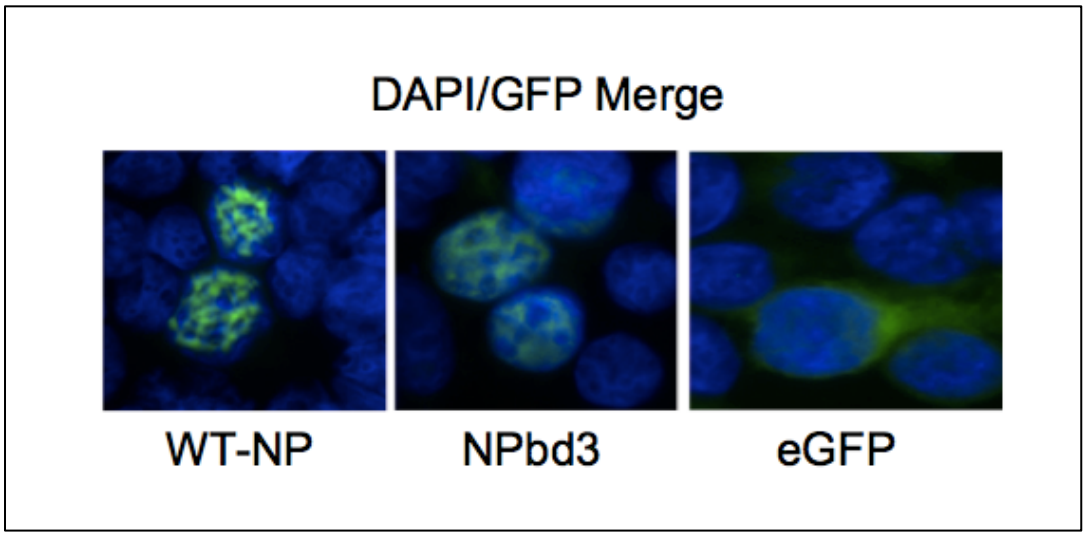

Figure 11. NPbd3 is Localized as WT-NP.

NP-GFP, NPbd3-GFP, or eGFP were expressed in cells grown on poly-L-Lysine cover slips. Cells were washed and fixed using a 1:1 methanol and acetone mixture. The coverslips were mounted onto glass slides using SouthernBiotech™ Dapi-Fluoromount-G™ Clear Mounting Media which stains the cell nucleus blue. Slides were observed on a Nikon ECLIPSE TE2000-U fluorescent microscope and images were captured with an Andor Clara DR-3446 camera using NIS-Elements AR software.

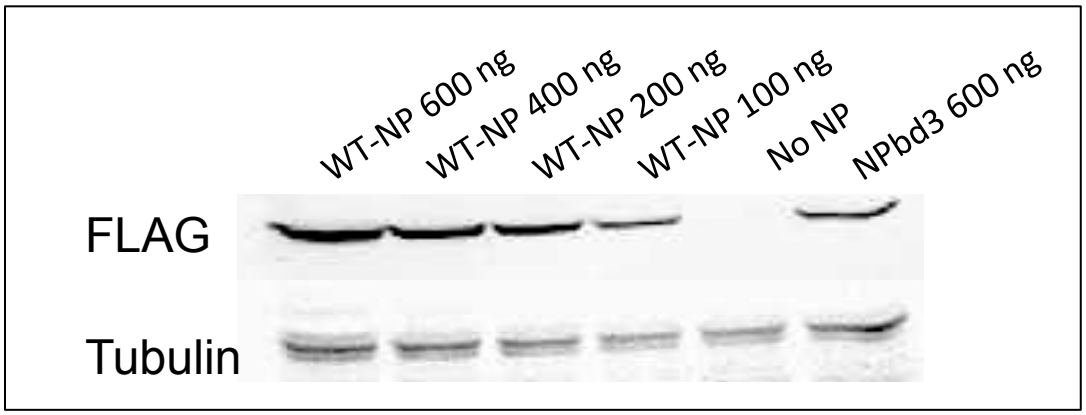

Figure 12. Low Levels of NP Support Viral Ribonucleoprotein Formation. Total protein from titration samples was isolated and run on a 10% SDS PAGE and transferred to nitrocellulose. The membrane was probed with anti-FLAG to identify NP and anti-Tubulin as the loading control.

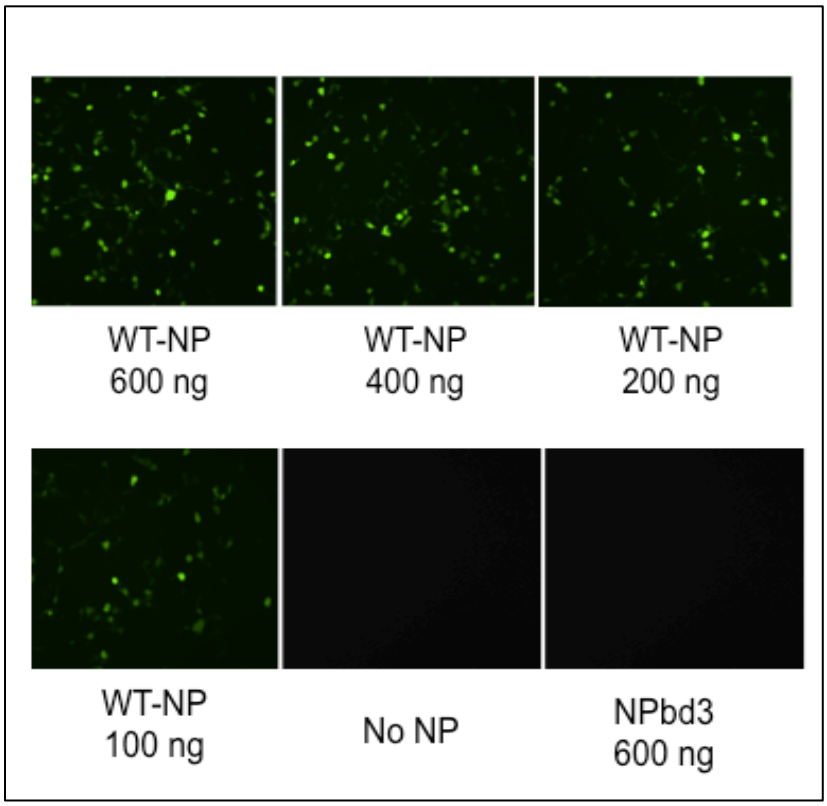

Figure 13. NP Titration Displays Activity at Lower Plasmid Concentration. Plasmids to express reconstituted vRNPs with GFP-M vRNA and either WT-NP, no NP, or NPbd3 at the concentrations listed above were transfected into 293T cells. 48 hours post transfection cells were observed for GFP-M expression. WT-NP (400 ng) represents the standard concentration used in our experiments and positive control while no NP is the negative control. GFP was visualized with a Nikon Eclipse TS100 (Nikon Intensilight C-HGFI for fluorescence) inverted microscope and images captured with the Nikon DS-Qi1Mc camera with NS Elements software.

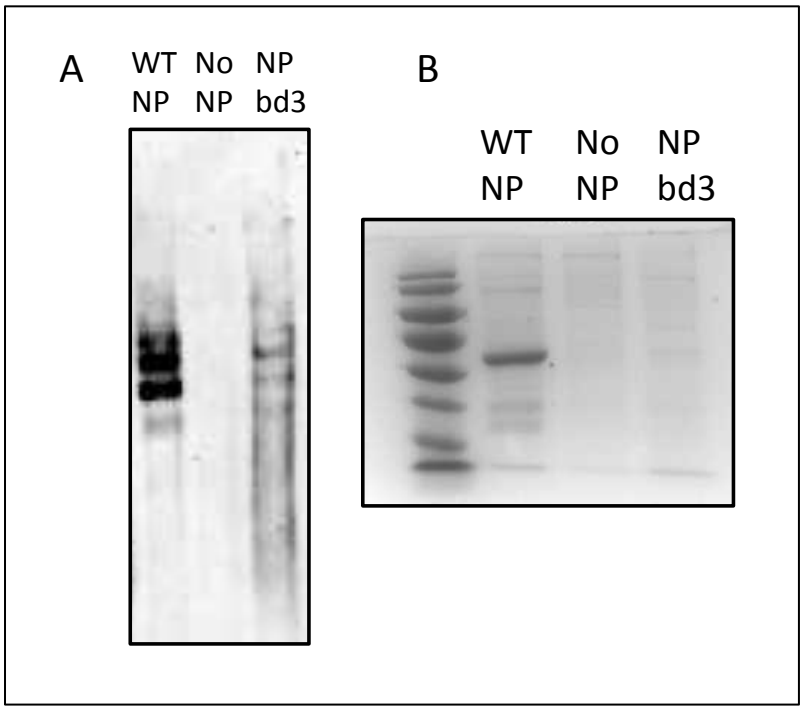

Figure 14. NPbd3 Maintains Nucleic Acid Binding.

A. WT-NP and NPbd3 were immunopurified using anti-FLAG agarose beads. Purified WT-NP and NPbd3 were incubated with biotin labeled single stranded DNA and separated on an 8% PAGE TBE non denaturing gel before transfer to nitrocellulose. Biotin ssDNA was detected by interaction with Streptavidin-HRP and ECL reagents. No NP samples serve as the negative control. B. Immunopurified WT-NP and NPbd3 were run on a 10% denaturing gel and stained with Coomassie Blue.

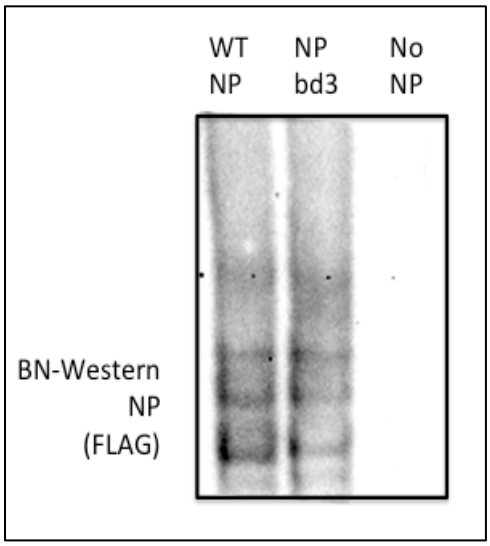

Figure 15. NPbd3 Forms Oligomers as WT-NP.

Blue Native Gel Electrophoresis was utilized to migrate protein extracts followed by western blot with anti-FLAG antibody to demonstrate NP oligomer formation. (Laura Newcomb and Jose Ramirez).

CHAPTER FOUR

NUCLEOPROTEIN BODY DOMAIN SINGLE MUTANT ANALYSIS

Background

To investigate the NP body domain further, single amino acid glycine substitution mutants were cloned, Y289G, K293G, E294G, Q308G, and N309G. This method was conducted to conclude whether a single amino acid substitution was solely responsible for the defect observed in NPbd3.

Viral Ribonucleoprotein Activity

Single amino acid mutants were analyzed for vRNP function by assessing GFP expression using our reconstituted vRNP expression system with GFP-M vRNA (Fig. 5). All five single NP mutants displayed activity similar to WT-NP (Fig. 16). Protein analysis showed the NP single mutants were expressed at levels similar to WT-NP (Fig. 17). RNA analysis of the M gene through reverse transcription using oligo-dT primers and qPCR revealed levels of viral mRNA expression with no statistical difference compared to WT-NP (Fig. 18). Therefore, our analysis of NP single substitutions within this region of the body domain revealed that all were nearly as functional as WT-NP, suggesting these accessible amino acids play a redundant role.

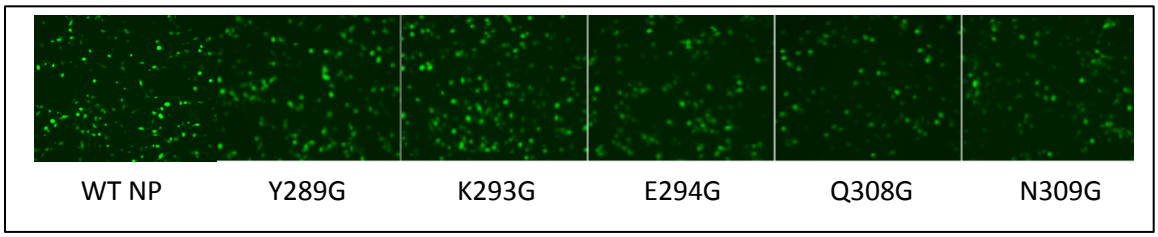

Figure 16. NP Single Amino Acid Mutants Result in Expression of Viral Protein. Cells expressing reconstituted vRNPs with GFP-M vRNA were visualized for GFP expression with a Nikon Eclipse TS100 (Nikon Intensilight C-HGFI for fluorescence) inverted microscope and images captured with the Nikon DS-Qi1Mc camera with NS Elements software.

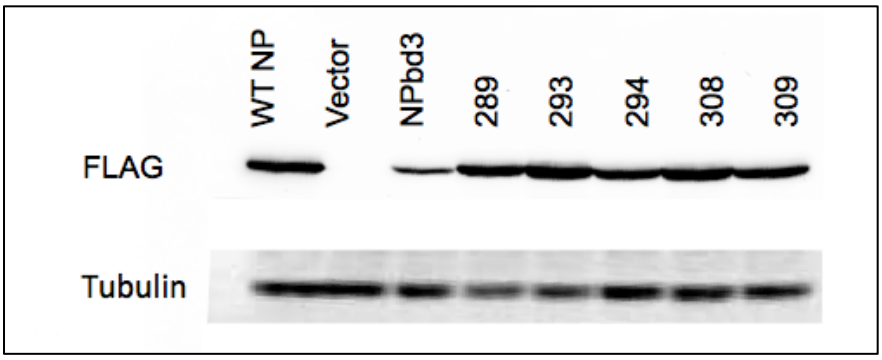

Figure 17. NP Single Mutants are Expressed as WT-NP.

Total protein was isolated from cells expressing reconstituted vRNPs with GFP-M vRNA template and WT-NP, no NP, or NP mutant. Total protein extract was separated on 10% SDS PAGE and transferred to nitrocellulose. WT-NP, NPbd3, and NP single mutants were detected with anti-FLAG. Anti-tubulin was used as loading control.

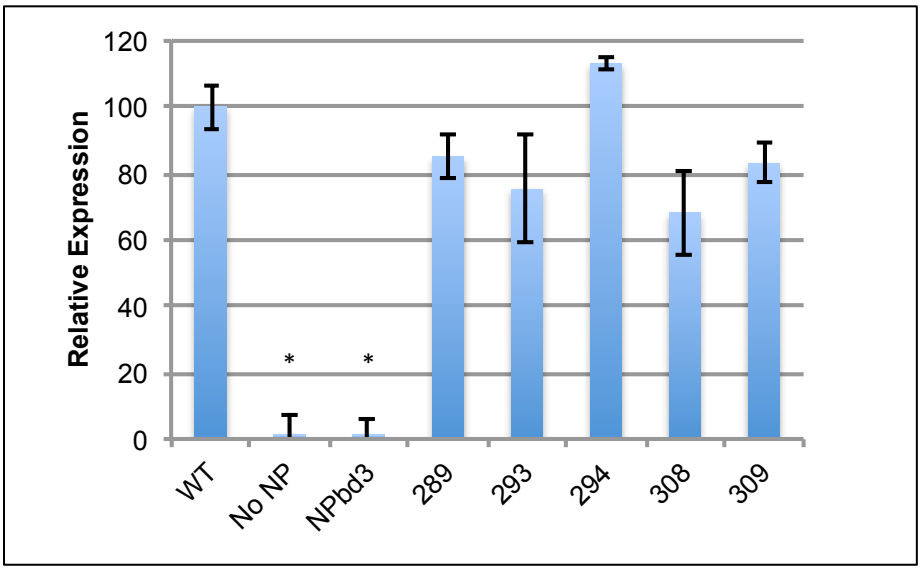

Figure 18. NP Single Mutants Show No Significant Defect in Viral RNA Expression.

RNA from cells expressing reconstituted vRNPs with FLAG-M vRNA and either WT-NP, no NP, NPbd3, or the single amino acid NP mutants were isolated. One microgram of RNA was treated with DNase before being reverse transcribed with oligo dT (mRNA) and analyzed through qPCR with primers targeting the M gene. qPCR reactions were carried out in triplicate. Significance was evaluated through t-test by comparing to WT-NP; asterisks indicate p-values <0.01.

CHAPTER FIVE

NUCLEOPROTEIN BODY DOMAIN DOUBLE MUTANT ANALYSIS

Background

Single amino acid substitutions within the region of NPbd3 resulted in functional proteins that acted as WT-NP. These results prompted the creation of combinational mutations consisting of two amino acid substitutions with the goal of identifying an NP double mutant with a significant defect in activity.

Viral Ribonucleoprotein Activity

Amino acid pairs were substituted within this region of the NP body domain to further define which residues contribute to the defect observed. Four body domain double mutants were constructed, Q308G/N309G, Y289G/E294G, Y289G/N309G, and K293G/E294G. The pairs of double mutants were designed based on the relative proximity of the two amino acids to each other using the NP crystal structure (Fig. 9). These double mutants were analyzed for vRNP function by assessing GFP expression using our reconstituted vRNP expression system with GFP-M vRNA (Fig. 5). All NP double mutants showed statistically less GFP expression than WT-NP (Fig. 19). Total protein analysis by Western blot revealed that all NP double mutants are expressed as WT-NP (Fig. 20). RNA analysis of the M gene through reverse transcription using oligo-dT primers and qPCR revealed a significant decrease in viral mRNA expression in all double mutants compared to WT-NP (Fig. 21). Analysis of NP double mutants supports the

defect in viral RNA expression observed with NPbd3 is likely caused by a combination of multiple accessible amino acids in the NP body domain.

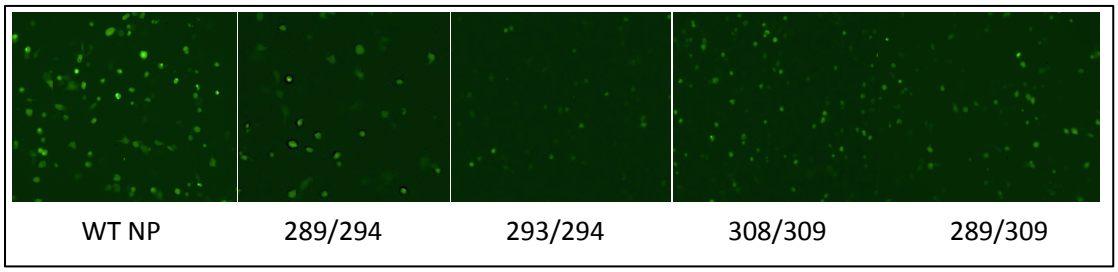

Figure 19. NP Double Amino Acid Mutants Result in Varied Expression of Viral Protein.

Cells expressing reconstituted vRNPs with GFP-M vRNA were visualized for GFP expression with a Nikon Eclipse TS100 (Nikon Intensilight C-HGFI for fluorescence) inverted microscope and images captured with the Nikon DS-Qi1Mc camera with NS Elements software.

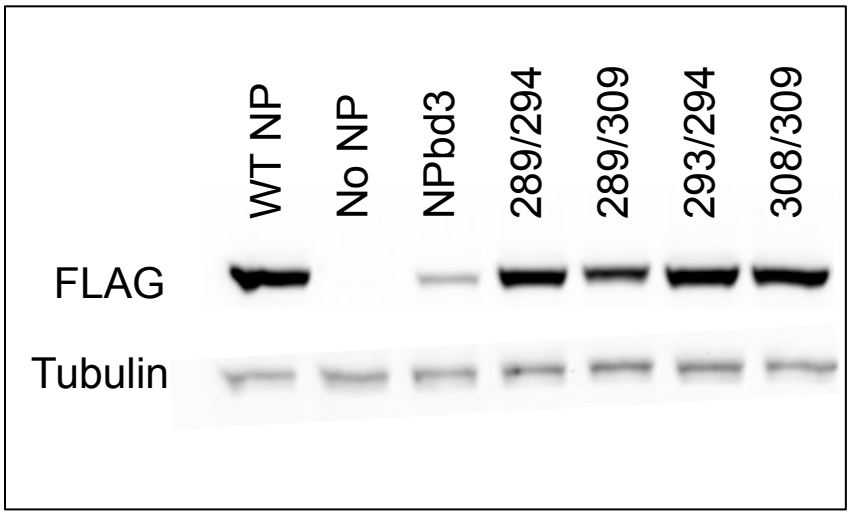

Figure 20. NP Double Mutants are Expressed as WT-NP.

Total protein was isolated from cells expressing reconstituted vRNPs with GFP-M vRNA template and the indicated NP mutant. Total protein extract was separated on 10% SDS PAGE and transferred to nitrocellulose. WT-NP, NPbd3, and NP double mutants were detected with anti-FLAG. Anti-tubulin was used as loading control.

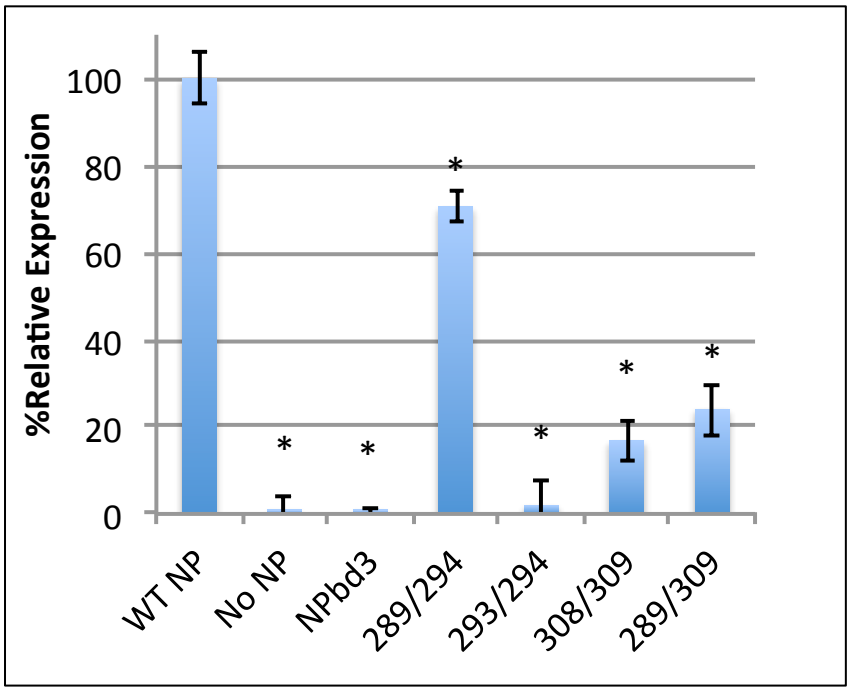

Figure 21. NP Double Amino Acid Mutants Show Defect in Viral RNA Expression. RNA from cells expressing reconstituted vRNPs with FLAG-M vRNA and either WT-NP, no NP, NPbd3, or the double amino acid NP mutants were isolated. One microgram of RNA was treated with DNase before being reverse transcribed with oligo dT (mRNA) and analyzed through quantitative PCR with primers targeting the M gene. qPCR reactions were carried out in triplicate. Significance was evaluated through t-test by comparing WT-NP; asterisks indicate p-values <0.02.

CHAPTER SIX

INTERACTION STUDIES OF NP AND PB2

In order to directly determine NPbd3 interaction with the viral polymerase co-immunoprecipitation from cellular extracts were performed. Since avian influenza virus passaged in human cells resulted in virus with one amino acid change at residue 309 of NP consistently paired with changes in amino acid 627 of the PB2 subunit of the RdRP (Danzy et. al., 2014), we focused our initial assessment on the NP-PB2 interaction. To facilitate studies with PB2, a C-terminal STREP tagged PB2 protein was constructed through cloning (Rameix-Welti et al., 2009). The construct was confirmed by sequencing and tested for activity in a reconstituted vRNP assay (Fig. 22). Additionally a Western blot was performed to identify the presence of the Strep epitope tag (Fig. 23). Although the insert of the plasmid was confirmed by sequencing several times, the STREP antibody never successfully bound to PB2 C-STREP.

An alternative approach was then taken using Anti-FLAG M2 Affinity Gel agarose beads for immunopurification and a PB2 antibody to assess NP and PB2 interaction. WT-NP and PB2, 293/294 NP and PB2, WT-NP alone, 293/294 NP alone, and PB2 alone were transfected in to 293T cells (Table 6). Immunopurified proteins were run on a denaturing gel, transferred to nitrocellulose and probed with anti-PB2 (Fig. 24). The blot was stripped and also probed with Anti-FLAG (Fig. 24). When comparing the eluted fraction of WT-NP/PB2 and 293/294/PB2 there is less PB2 pulled down in the presence of the

293/294 NP mutant. The amount of PB2 pulled down and eluted in the 293/294 NP with PB2 sample is similar to the PB2 alone, which serves as a background control. However, the amount of eluted 293/294 NP mutant is also less than WT-NP. No definitive conclusions can be drawn from this trial but this work serves as preliminary interaction data and demonstrates we should be able to repeat this assay and obtain conclusive and repeatable results to determine whether or not NP-PB2 interaction is disrupted with NP mutants within the body domain.

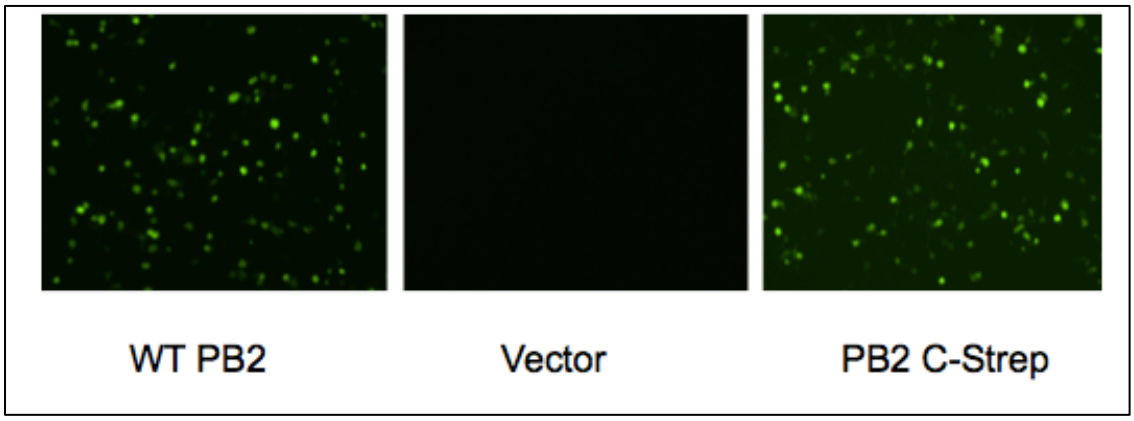

Figure 22. PB2 C-STREP Activity.

Cells expressing reconstituted vRNPs with WT PB2, no PB2, or PB2 C-STREP with GFP-M vRNA were visualized for GFP expression with a Nikon Eclipse TS100 (Nikon Intensilight C-HGFI for fluorescence) inverted microscope and images captured with the Nikon DS-Qi1Mc camera with NS Elements software.

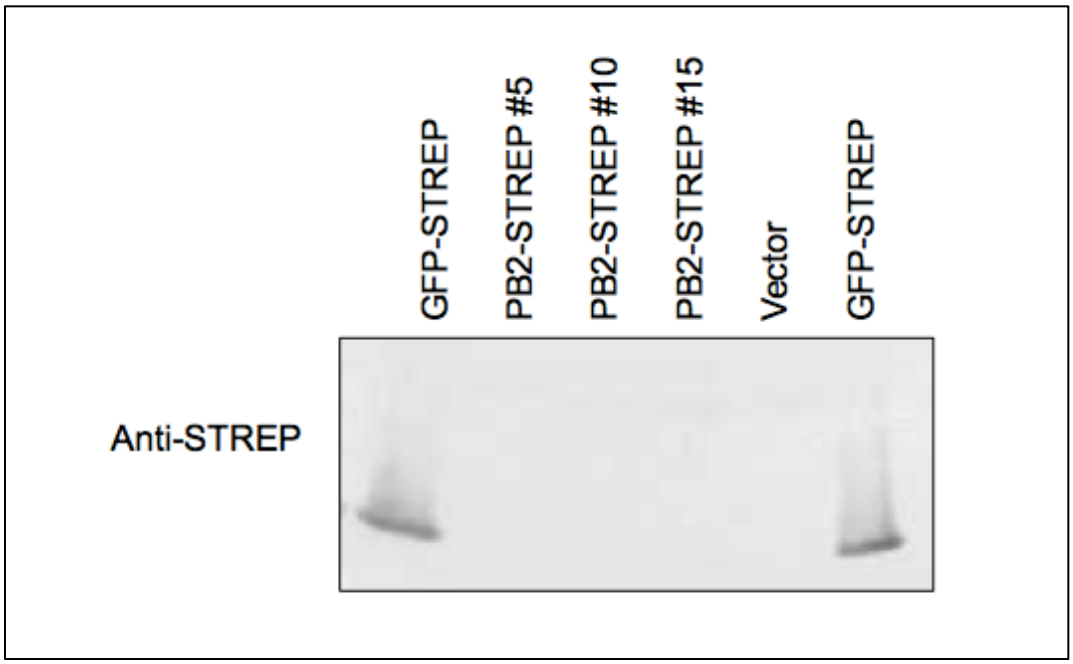

Figure 23. STREP Epitope Not Detected in Western Blot.

Total protein was isolated from cells expressing GFP-STREP control protein, PB2 C-STREP candidates, or vector. Total protein extract was separated on 10% SDS PAGE and transferred to nitrocellulose. STREP tagged proteins were detected with anti-STREP.

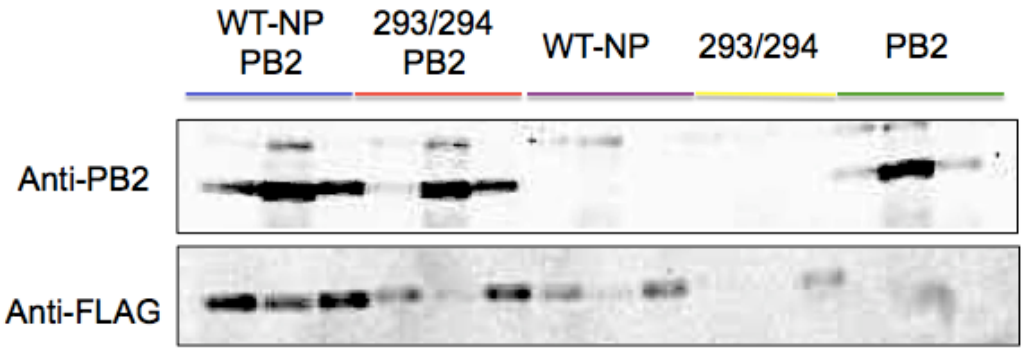

Figure 24. Co-Immunoprecipitation of NP and PB2.

Cells expressing WT-NP and PB2, 293/294 NP and PB2, WT-NP alone, 293/294 alone, or PB2 alone were fractionated and immunopurified. Eluate, flow through, and beads from each sample were run on a 10% SDS PAGE and transferred to nitrocellulose. The membrane was probed with anti-PB2, stripped, and probed with anti-FLAG. The three lanes of each sample contain the eluate, flow-through, and beads (left to right).

CHAPTER SEVEN

SUMMARY AND DISCUSSION

Mutational analysis of the NP body domain revealed a region of five amino acids that is essential for viral gene expression. NPbd3 encodes glycine at 5 amino acids within an accessible region of the NP body domain. Cellular fractionation and Western blot, in addition to NP-GFP fusions and fluorescence, confirm NPbd3 was expressed and localized as WT-NP (Fig. 10 and 11). Gel shift (EMSA) with purified NP protein confirm NPbd3 bound nucleic acids as WT-NP (Fig. 14). Blue Native Gel Electrophoresis demonstrated NPbd3 oligomerized (Fig. 15). Although NPbd3 was expressed, localized, and bound nucleic acid as WT-NP, we found NPbd3 was defective for RNA expression in reconstituted vRNPs and cRNPs as evaluated by reverse transcription and quantitative polymerase chain reaction (RT-qPCR).

To investigate this region of the NP body domain further, single and double amino acid mutations were cloned. Analysis of NP single mutants revealed that all were nearly as functional as WT-NP for RNA expression in reconstituted vRNPs, suggesting these accessible amino acids in the NP body domain play a redundant role (Fig. 18). However, four different combinations of two amino acid mutations resulted in NP double mutants that displayed a significant defect in RNA expression in reconstituted vRNPs, confirming these accessible amino acids in the NP body domain play a significant role for viral RNA synthesis (Fig. 21). The greatest defect in mRNA synthesis observed was in

double mutant 293/294, followed by 308/309, 289/309, and 289/294. Although amino acid 293 is variable and 294 is conserved, a mutation at 294 alone was not sufficient to cause a defect and the defect observed with 289/294 was only minimal. In our assays, 294 coupled with a change at 293 resulted in the greatest observed defect in RNA synthesis. The glutamic acid at 294 has a negative charge while the lysine at 293 is positively charged. Perhaps these opposite charged residues provide an internal interaction important for supporting the activity occurring at this domain. Future mutational analysis to substitute a negatively charged residue at 293 and a positively charged residue at 294 may provide more insight in to the interactions in and around 293/294. The tyrosine at residue 289, glutamine at residue 308, and asparagine at residue 309 are moderately to highly conserved and polar: substituting a glycine at any two of these residues leads to a defect in mRNA synthesis.

The body domain region designated for mutagenesis in NPbd3 was selected for probable interaction with the RdRP based on mini-replicon images (Coloma et al., 2009). While 294 and 293 may be involved in an internal NP interaction, we hypothesize that disruption of an essential NP interaction with the RdRP is the explanation for the RNA defect observed with mutations at 308/309 and 289/309. In support of this, avian influenza virus passaged in human cells resulted in virus with one amino acid change at residue 309 of NP consistently paired with specific changes in amino acid 627 of the PB2 subunit of the RdRP (Danzy et. al., 2014). The double mutant displaying the most significant defect in

RNA synthesis, 293/294, was used in co-immunopreciptation trials with PB2 (Fig. 24). Since this double mutant may not represent NP interaction with the polymerase, this experiment will be repeated with inclusion of analysis of 308/309 and 289/309 in order to make a conclusion on the interaction between our body domain mutants and PB2. Future experiments are focused on obtaining a better co-immunoprecipitation gel image and running a blue native gel of vRNPs with small templates to assess vRNP formation directly as in Sanchez et al., 2014.

I reason that this accessible body domain of NP is an important NP interaction surface and small molecule inhibitors could block access to this NP interaction, making this region a viable antiviral target. Indeed, two amino acids in this NP body domain, 289 and 309, comprise a novel groove implicated in binding the small molecule inhibitor nucleozin (Kao et. al., 2010). The influenza A(H1N1)pdm09 strains contained a rare polymorphism at residue 289 (Kao et. al., 2010). Instead of a tyrosine, these H1N1 strains contain a histidine at amino acid 289. Tyrosine has a large hydrophobic side chain while histidine has a smaller and positively charged side chain. This change likely disrupts the aromatic ring stacking between nucleozin and the tyrosine at 289 (Kao et. al., 2010). Beyond this, another compound, FA-10 has shown efficacy against the A(H1N1)pdm09 strains but less activity toward wild-type WSN virus (Kao et. al., 2010). These studies show that optimization of compounds targeting this domain could lead to an effective antiviral drug. The work presented here has defined

this domain with greater clarity, providing evidence that the polar amino acids 289, 308, and 309 provide one target while the charged interaction at 293 and 294 is likely a separate target; perhaps both regions of the domain can be targeted in a combinational therapeutic approach. This thesis demonstrates that disruption of this accessible domain should block viral RNA expression and support additional studies of novel antivirals targeting this conserved NP body domain.

CHAPTER EIGHT

MATERIALS AND METHODS

Nucleoprotein Body Domain Mutant Construction

First Step PCR

Polymerase chain reactions (PCR) were carried out in a total of 50 µl with Thermo Scientific Phusion High-Fidelity DNA polymerase master mix at a 1X concentration, 50 picomoles (pmol) of each primer, 200 ng of pcDNA NP-FLAG DNA, and sterile water up to volume.

Table 2. First Step PCR Conditions

Reaction	Primers	Cycling Conditions
Reaction A: Large fragment	5' EcoRI NP and 3' Mutant primer	Initial denaturation: 95 °C for 60 seconds. Denature: 95 °C for 30 seconds. Anneal: 60 °C for 40 seconds. Extend: 72 °C for 150 seconds. 25 cycles.
Reaction B: Small Fragment	5' Mutant primer and 3' Xbalstop1XFLAG	Same as above.

Table 3. Primer Sequences

Construct Name	Primer Name	Sequence (5' to 3')
NPbd3	NP5X289-309-F	GGCGACTTCGAAGGAGGAGGATACTCTTTAGTGGGAATAGACCCTTTCAAACTACTTGGAGGCAGCCAAG
	NP5X289-309-R	GCCTCCAAGTAGTTTGAAAGGGTCTATTCCCACTAAAGAGTATCCTCCTCCGAAGTCGCCCCCACTG
Y289G	289G-F	GCCAGTGGG**GGC**GACTTCG
	289G-R	CGAAGTC**GCC**CCCACTGGC
K293G	293G-F	TACGACTTCGAA**GGA**GAGGGATACTCT
	293G-R	AGAGTATCCCTC**TCC**TTCGAAGTCGTA
E294G	294G-F	GACTTCGAAAAA**GGA**GGATACTC
	294G-R	GAGTATCC**TCC**TTTTTCGAAGTC
Q308G	308G-F	CCTTTCAAACTACTT**GGA**AACAGC
	308G-R	GCTGTT**TCC**AAGTAGTTTGAAAGG
N309G	309G-F	CTACTTCAA**GGC**AGCCAAGTATAC
	309G-R	GTATACTTGGCT**GCC**TTGAAGTAG
Y289G/E294G	289/294-F	GGG**GGC**GACTTCGAAAAA**GGA**GG
	289/294-R	CC**TCC**TTTTTCGAAGTC**GCC**CCC
K293G/E294G	293/294-F	TACGACTTCGAA**GGAGGA**GGATACTCTTTAGTGGGAATAGACCCTTTCAAACTACTTCAAAAC
	293/294-R	GTTTTGAAGTAGTTTGAAAGGGTCTATTCCCACTAAAGAGTATCC**TCCTCC**TTCGAAGTCGTA
Q308G/N309G	308/309-F	CCTTTCAAACTACTT**GGAGGC**AGC
	308/309-R	GCT**GCCTCC**AAGTAGTTTGAAAGG
Y289G/Q309G	289/309-F	**GGC**GACTTCGAAAAAGAGGGATACTCTTTAGTGGGAATAGACCCTTTCAAACTACTTCAA**GGC**
	289/309-R	**GCC**TTGAAGTAGTTTGAAAGGGTCTATTCCCACTAAAGAGTATCCCTCTTTTTCGAAGTC**GCC**
Restriction Enzyme End Primers	Primer Name	Sequence (5' to 3')
EcoRI	5' EcoRI NP	TATGAATTCATGGCGTCCCAAGGC
XbaI	3' Xbalstop1 XFLAG	GACTCTAGATTAACCGTCATGGTCTTTGTAGTCCGCCGCATTGTCGTACTCC

Agarose Gel Extraction. PCR products were run on a 1% agarose gel for 55 minutes at 120 volts (V) and 400 milliamps (mA) to separate any remaining template DNA from desired product. The QIAquick® Gel Extraction protocol was followed except for the addition of isopropanol.

Second Step PCR

The next step in the construction required the combination of the small and large DNA fragments with the addition of restriction enzyme encoded end primers to obtain the entire desired insert. PCR reactions were carried out in a total of 50 µl with Thermo Scientific Phusion High-Fidelity DNA polymerase master mix at a 1X concentration, 100 ng of the large fragment, 70 ng of the small fragment, and 50 pmol of each primer (5' EcoRI NP and 3' Xbalstop1XFLAG) which was added after 10 cycles of PCR. The ratio for the amount of each fragment needed for PCR was calculated by the following equation: (100ng Large fragment X Size of Small fragment)/ Size of Large fragment= ng of small fragment for every 100ng large fragment. The second PCR cycling conditions were as follows: Initial Denaturation: 95 °C for 60 seconds. Denature: 95 °C for 30 seconds. Anneal: 60 °C for 40 seconds. Extend: 72 °C for 150 seconds. 25 cycles. (Primers added after 10 cycles).

Confirmation Gel and PCR Purification. Five µl of the 2nd PCR reaction products, also referred to as the 'insert', were loaded on a 1% agarose gel and run for 55 minutes at 120V and 400mA. The remaining 45 µl of the PCR products

were purified following the QIAquick® PCR Purification protocol with an elution in 30 µl.

Digest with EcoRI and XbaI. 140 ng of the insert and 500 ng of pcDNA vector were separately digested with EcoRI (1:20 dilution), XbaI (1:20 dilution), 1X Tango buffer, and water up to volume. The reactions were incubated overnight at 37 °C. The pcDNA vector was then phosphatase treated with Antarctic Phosphatase (1:10 dilution) and Antarctic Phosphatase buffer (1:10 dilution) for 30 minutes at 37 °C. The insert and vector were heat inactivated at 80 °C for 20 minutes.

Ligation. Ligation reactions were carried out at the following vector to insert ratios: 1:1, 1:3, and 1:5. A vector only negative control was included. Each reaction tube included digested insert and vector DNA (except vector only control), T4 DNA Ligase (1:10 dilution), T4 DNA Ligase Buffer (1:10 dilution), and water up to volume. The reaction was incubated overnight at 4 °C.

Transformation. Ligated plasmids were transformed into chemically competent *E. coli* cells. In addition to the 1:1, 1:3, 1:5, and vector ligations, a no DNA control and a positive pUC19 control were also transformed. The manufacturer's protocol was followed for TransMax FB5α Competent Cells-10E9 at a smaller volume of 25 µl of cells and 250 µl of S.O.C. medium. The transformed cells were spread onto Luria-Bertani (LB) agar plates containing ampicillin (at 100 mg/mL) and incubated over night at 37°C.

Colony PCR

Candidate colonies on transformation plates were screened for the plasmid of interest using colony PCR. Individual colonies were picked with a 100 µl pipet tip and used to introduce bacterial cells to a PCR master mix (50 pmol 5' EcoRI NP and 3' Xbalstop1XFLAG restriction enzyme end primers, 1X master mix for Promega *Taq* polymerase, and water) and also LB AMP liquid media (grown at 37°C overnight). The following PCR conditions were used: Initial Denaturation: 95°C for 60 seconds. Denature: 95°C for 30 seconds. Anneal: 60°C for 40 seconds. Extend: 72°C for 150 seconds. 30 cycles. WT-NP was used as a positive control, while pcDNA vector was used as a negative control. The PCR products were run on a 1% agarose gel for 55 minutes at 120 V and 400 mA. Candidates demonstrating a similar pattern to WT-NP were miniprepped using the QIAprep® Spin Miniprep protocol.

Diagnostic Digest

Candidate plasmids were subjected to a diagnostic digest. 400 ng of DNA was incubated with EcoRI (1:20 dilution), XbaI (1:20 dilution), 1X buffer, and water at 37°C for one hour. WT-NP was used as a positive control, while pcDNA vector was used as a negative control. Digested DNA was run on a 1% agarose gel for 55 minutes at 120 V and 400 mA. Candidates displaying a pattern similar to WT-NP were sent out for sequencing using flanking and internal primers. Sequence analysis was carried out using Basic Local Alignment Search Tool

(BLAST). Plasmids containing the desired mutation were prepared for long term storage in 15% glycerol and stored at -80 °C.

PB2 C-STREP

Linearization of Template DNA

2,000 ng of pcDNA PB2 was digested with BamHI at a 1:10 dilution at 37 °C for over night in order to linearize the template to be used in the first round of PCR. The digest was confirmed by migration on a 1% agarose gel for 50 minutes at 120 V and 400 mA.

Table 4. Primers for PB2 C-STREP Construction

Primer Name	Sequence (5' to 3')
BamHIPB2F	CGCGGATCCATGGAAAGAATAAAAGAACTACGGAATCT GATGTCGC
XbalStrepPB2R	ATATCTAGATTATTTCTCAAATTGTGGATGAGACCAAGC TGCTGCATTGATGGCCATCCG

PB2 C-STREP PCR

PCR reactions were carried out in a total of 50 µL with Thermo Scientific Phusion High-Fidelity DNA polymerase master mix at a 1X concentration, 50 pmol of each primer, 200 ng of linearized pcDNA PB2 DNA, and sterile water up to volume. PB2 C-STREP cycling conditions were as follows: Initial Denaturation: 95 °C for 60 seconds. Denature: 95 °C for 30 seconds. Anneal: 70 °C for 40 seconds. Extend: 72 °C for 150 seconds. 25 cycles.

PCR product gel extraction, digest, ligation, transformation, colony PCR, diagnostic digest, and sequencing were performed in the same manner as the NP plasmid constructs. BamHI and XbaI restriction enzyme sites were utilized for PB2 C-STREP construction.

Reconstituted Viral Ribonucleoprotein Activity Assay

Cells

293T human embryonic kidney cells were purchased from American Tissue Culture Collection and maintained at 37 ˚C with 5% CO_2 in DMEM with 10% FBS.

Reconstituted Ribonucleoprotein Expression System

In order to reconstitute the influenza RNP expression system, pcDNA expression vectors of PB1, PB2, PA, and wildtype or mutant NP were transfected into 293T cells. A pHH21 GFP-MvRNA or pHH21 McRNA expression vector was used to express the coding RNA. Cellular RNA polymerase I drives expression of the cRNA or vRNA template from pHH21 encoding plasmids. Cellular RNA polymerase II drives expression of viral mRNAs from pcDNA3 encoding

plasmids.

Table 5. Reconstituted Ribonucleoprotein Expression System

Plasmid	Nanograms of DNA (6 well plate)
pcDNA PB1	400
pcDNA WT PB2	400
pcDNA PA	200
pcDNA WT-NP OR No NP (Vector) OR pcDNA NP mutant	600
pHH21 GFP MvRNA OR pHH21 McRNA	400

Transfection

Preparation for transfection began by incubating a lipid-based Trans-IT reagent (DNA to reagent ratio of 1:3 per plasmid mixture) with 250 µl of serumfree media (per plasmid mixture) for five minutes at room temperature. The transfection mixture was then added to the plasmid mixture containing tubes, flicked to mix, and incubated for 15 minutes at room temperature. The mixture of plasmids, reagent, and media were then added drop wise into 293T cells at 65 percent confluency. Cells were incubated in a tissue culture incubator for 48 hours.

Green Fluorescent Protein Visualization

Cells were observed for GFP-M expression 48 hours post transfection. WT-NP was the positive control while no NP is the negative control. GFP was visualized with a Nikon Eclipse TS100 (Nikon Intensilight C-HGFI for fluorescence) inverted microscope and images captured with the Nikon DS-Qi1Mc camera with NS Elements software.

Cell Collection

Cells were collected and pelleted by centrifugation 48 hours post-transfection. Proteins were isolated through either total protein isolation or cellular fractionation.

Total Protein Isolation

Cell pellets were resuspended in RIPA Lysis Buffer (25 mM HCl pH 7.6, 150 mM NaCl, 1% deoxycholate, 0.1% SDS) containing protease inhibitors and lysed using a Fisher Scientific Sonic Dismembrator for 10 pulses at 30%, output 3-4. Proteins were denatured using 1X SDS protein loading dye and boiling for five minutes. Proteins were separated on a 10% sodium dodecyl sulfate polyacrylamide gel electrophoresis (SDS PAGE) and transferred to nitrocellulose. All NP constructs contain a FLAG epitope tag and were detected using anti-FLAG. Anti-tubulin was used to confirm even protein loading when evaluating total protein.

Cellular Fractionation

Cells were fractionated using 10% NP-40 non-ionic detergent to break open cellular plasma membrane while keeping the nuclear membranes intact. Microscopy was used to confirm disrupted plasma membranes and intact nuclei. The nuclei were pelleted by centrifugation and sonicated for 30 pulses at 30% to bust the nuclear membrane. Both nuclear and cytoplasmic fractions were clarified by high-speed centrifugation.

Immunopurification

The nuclear fraction of cells transfected with WT-NP, NPbd3, or No NP were incubated with Anti-FLAG M2 Affinity Gel agarose beads (Sigma-Aldrich), incubated overnight at 4°C with rotation, washed five times in RSB (reticulocyte standard buffer: 10mM Tris HCl pH 7.5, 10mM KCl, 1.5mM $MgCl_2$) + 0.2% NP-40, and eluted with 150 ng/ul 3X FLAG peptide (APEXBIO). The elutant was separated on a 10% SDS PAGE and stained with Coomassie Blue overnight to check purity.

Gel Shift

Immunopurified proteins were incubated with 20 picomoles of biotin-labeled ssDNA for 20 minutes at room temperature and mixed with 2.5% glycerol for loading. The protein-DNA samples were run on an 8% TBE non-denaturing PAGE in 4°C, followed by transfer to nitrocellulose and Western blotting. The membrane was probed with Streptavadin-HRP (1:3,000) and Pierce ECL reagents were used to detect the biotin labeled ssDNA.

Blue Native Polyacrylamide Gel Electrophoresis

Total protein from WT-NP, NPbd3, or no NP transfected cells were run on a 6% 1D Blue Native PAGE (Lin et al., 2012) and transferred on to nitrocellulose. The blot was probed with anti-FLAG to detect WT-NP and NPbd3.

RNA Isolation

Total RNA was isolated with Trizol (Invitrogen), following the manufacturer's protocol. RNA concentration and purity of samples was determined at OD_{260} and OD_{280} using a NanoDrop ND1000 Nanospectrophotometer (Thermo Fischer Scientific). Integrity of rRNA was evaluated on a 1% bleach/1% agarose gel (Aranda et. al., 2012).

RTqPCR

2.5 µg of RNA was DNase treated. 1 µg was reverse transcribed using Promega AMV reverse transcription system following the manufacturer's protocol. 1 µg was used in the negative control reaction, lacking the AMV reverse transcriptase enzyme to control for DNA contamination. Oligo dT (mRNA) or vRNA specific primers (vRNA) were used in the RT reaction to produce cDNA. Real time quantitative PCR using an Applied Biosystems SYBR Select Master Mix was performed on cDNA with primers targeting the influenza M gene. qPCR reactions were carried out in triplicate using the AB Step One qPCR machine. Significance was evaluated through t-test by comparing WT-NP with no NP or NPbd3 both reporting significance with p-values <0.02.

Green Fluorescent Protein Fusion Location

Plasmids expressing NP-GFP, NPbd3-GFP, or eGFP were transfected into 293T cells grown on poly-L-Lysine cover slips. 48 hours post transfection the cells were washed and fixed using a 1:1 methanol and acetone mixture. The coverslips were mounted onto glass slides using SouthernBiotech™ Dapi-Fluoromount-G™ Clear Mounting Media, which stains the cell nucleus blue. Slides were observed on a Nikon ECLIPSE TE2000-U fluorescent microscope and images were captured with an Andor Clara DR-3446 camera using NIS-Elements AR software. Plasmids NP-GFP and NPbd3-GFP were constructed by Alan Santana

Testing PB2 C-STREP for Activity

293T cells were transfected following the guidelines in Table 5. GFP images were captured using Nikon Eclipse TS100 (Nikon Intensilight C-HGFI for fluorescence) inverted microscope and images captured with the Nikon DS-Qi1Mc camera with NS Elements software. Total protein was isolated and separated on a 10% SDS gel and transferred to nitrocellulose. PB2 C-strep was detected using an anti-STREP antibody (IBA-LifeSciences).

Co-Immunoprecipitation

293T cells were transfected according to Table 6. Cells were collected, fractionated, and immunopurified as described above. Eluted proteins were run on a 10% SDS PAGE, transferred to nitrocellulose, and probed with anti-PB2 (GeneTex). The blots were stripped and probed again with anti-FLAG.

Table 6. Co-Immunoprecipitation Transfection

Sample	NP amount	PB2 amount
WT-NP/PB2	1,000 ng	9,000 ng
293:294/PB2	1,000 ng	9,000 ng
WT-NP only	1,000 ng	0
293:294 only	1,000 ng	0
PB2 only	0	9,000 ng

REFERENCES

Abed, Y., Goyette, N., & Boivin, G. (2005). Generation and characterization of recombinant influenza A (H1N1) viruses harboring amantadine resistance mutations. *Antimicrobial agents and chemotherapy*, *49*(2), 556-559.

Amorim, M. J., Kao, R. Y., & Digard, P. (2013). Nucleozin targets cytoplasmic trafficking of viral ribonucleoprotein-Rab11 complexes in influenza A virus infection. *Journal of virology*, *87*(8), 4694-4703.

Aranda, P. S., LaJoie, D. M., & Jorcyk, C. L. (2012). Bleach gel: a simple agarose gel for analyzing RNA quality. *Electrophoresis*, *33*(2), 366-369.

Arranz, R., Coloma, R., Chichón, F. J., Conesa, J. J., Carrascosa, J. L., Valpuesta, J. M., ... & Martín-Benito, J. (2012). The structure of native influenza virion ribonucleoproteins. *Science*, *338*(6114), 1634-1637.

Avalos, R. T., Yu, Z., & Nayak, D. P. (1997). Association of influenza virus NP and M1 proteins with cellular cytoskeletal elements in influenza virus-infected cells. *Journal of virology*, *71*(4), 2947-2958.

Baz, M., Abed, Y., Papenburg, J., Bouhy, X., Hamelin, M. È., & Boivin, G. (2009). Emergence of oseltamivir-resistant pandemic H1N1 virus during prophylaxis. *New England Journal of Medicine*, *361*(23), 2296-2297.

Beaton, A. R., & Krug, R. M. (1986). Transcription antitermination during influenza viral template RNA synthesis requires the nucleocapsid protein and the

absence of a 5'capped end. *Proceedings of the National Academy of Sciences*, *83*(17), 6282-6286.

Biswas, S. K., Boutz, P. L., & Nayak, D. P. (1998). Influenza virus nucleoprotein interacts with influenza virus polymerase proteins. *Journal of virology*, *72*(7), 5493-5501.

Centers for Disease Control and Prevention (1). http://www.cdc.gov/mmwr/preview/mmwrhtml/mm5929a2.htm.

Centers for Disease Control and Prevention (2). http://www.cdc.gov/flu/pastseasons/0910season.htm.

Centers for Disease Control and Prevention (3). http://www.cdc.gov/flu/about/qa/antiviralresistance.htm.

Chen, W., Calvo, P. A., Malide, D., Gibbs, J., Schubert, U., Bacik, I., ... & Henklein, P. (2001). A novel influenza A virus mitochondrial protein that induces cell death. *Nature medicine*, *7*(12), 1306-1312.

Chen, Y., Liang, W., Yang, S., Wu, N., Gao, H., Sheng, J., ... & Li, Y. (2013). Human infections with the emerging avian influenza A H7N9 virus from wet market poultry: clinical analysis and characterisation of viral genome. *The Lancet*, *381*(9881), 1916-1925.

Cianci, C., Gerritz, S. W., Deminie, C., & Krystal, M. (2013). Influenza nucleoprotein: promising target for antiviral chemotherapy. *Antiviral Chemistry and Chemotherapy*, *23*(3), 77-91.

Coloma, R., Valpuesta, J. M., Arranz, R., Carrascosa, J. L., Ortín, J., & Martín-Benito, J. (2009). The structure of a biologically active influenza virus ribonucleoprotein complex. *PLoS Pathog*, *5*(6), e1000491.

Cros, J. F., García‐Sastre, A., & Palese, P. (2005). An unconventional NLS is critical for the nuclear import of the influenza A virus nucleoprotein and ribonucleoprotein. *Traffic*, *6*(3), 205-213.

Danzy, S., Studdard, L. R., Manicassamy, B., Solorzano, A., Marshall, N., García-Sastre, A., ... & Lowen, A. C. (2014). Mutations to PB2 and NP proteins of an avian influenza virus combine to confer efficient growth in primary human respiratory cells. *Journal of virology*, *88*(22), 13436-13446.

Davis, A. M., Chabolla, B. J., & Newcomb, L. L. (2014). Emerging antiviral resistant strains of influenza A and the potential therapeutic targets within the viral ribonucleoprotein (vRNP) complex. *Virology journal*, *11*(1), 1.

Davis, A. R., Bos, T. J., & Nayak, D. P. (1983). Active influenza virus neuraminidase is expressed in monkey cells from cDNA cloned in simian virus 40 vectors. *Proceedings of the National Academy of Sciences*, *80*(13), 3976-3980.

Deng, T., Vreede, F. T., & Brownlee, G. G. (2006). Different de novo initiation strategies are used by influenza virus RNA polymerase on its cRNA and viral RNA promoters during viral RNA replication. *Journal of virology*, *80*(5), 2337-2348.

Deyde, V. M., Sheu, T. G., Trujillo, A. A., Okomo-Adhiambo, M., Garten, R., Klimov, A. I., & Gubareva, L. V. (2010). Detection of molecular markers of

drug resistance in 2009 pandemic influenza A (H1N1) viruses by pyrosequencing. *Antimicrobial agents and chemotherapy*, *54*(3), 1102-1110.

Dias, A., Bouvier, D., Crépin, T., McCarthy, A. A., Hart, D. J., Baudin, F., ... & Ruigrok, R. W. (2009). The cap-snatching endonuclease of influenza virus polymerase resides in the PA subunit. *Nature*, *458*(7240), 914-918.

Dubois, J., Terrier, O., & Rosa-Calatrava, M. (2014). Influenza viruses and mRNA splicing: doing more with less. *MBio*, *5*(3), e00070-14.

Fetcher, P., Mingay, L., Sharps, J., Chambers, A., Fodor, E., & Brownlee, G. G. (2003). Two aromatic residues in the PB2 subunit of influenza A RNA polymerase are crucial for cap binding. *Journal of Biological Chemistry*, *278*(22), 20381-20388.

Fukuoka, M., Minakuchi, M., Kawaguchi, A., Nagata, K., Kamatari, Y. O., & Kuwata, K. (2012). Structure-based discovery of anti-influenza virus A compounds among medicines. *Biochimica et Biophysica Acta (BBA)-General Subjects*, *1820*(2), 90-95.

Furuta, Y., Gowen, B. B., Takahashi, K., Shiraki, K., Smee, D. F., & Barnard, D. L. (2013). Favipiravir (T-705), a novel viral RNA polymerase inhibitor. *Antiviral research*, *100*(2), 446-454.

Furuta, Y., Takahashi, K., Fukuda, Y., Kuno, M., Kamiyama, T., Kozaki, K., ... & Narita, H. (2002). In vitro and in vivo activities of anti-influenza virus compound T-705. *Antimicrobial agents and chemotherapy*, *46*(4), 977-981.

Gao, R., Cao, B., Hu, Y., Feng, Z., Wang, D., Hu, W., ... & Xu, X. (2013). Human infection with a novel avian-origin influenza A (H7N9) virus. *New England Journal of Medicine*, *368*(20), 1888-1897.

Gerritz, S. W., Cianci, C., Kim, S., Pearce, B. C., Deminie, C., Discotto, L., ... & Zhai, W. (2011). Inhibition of influenza virus replication via small molecules that induce the formation of higher-order nucleoprotein oligomers. *Proceedings of the National Academy of Sciences*, *108*(37), 15366-15371.

González, S., & Ortín, J. (1999). Characterization of influenza virus PB1 protein binding to viral RNA: two separate regions of the protein contribute to the interaction domain. *Journal of virology*, *73*(1), 631-637.

González, S., Zürcher, T., & Ortín, J. (1996). Identification of two separate domains in the influenza virus PB1 protein involved in the interaction with the PB2 and PA subunits: a model for the viral RNA polymerase structure. *Nucleic acids research*, *24*(22), 4456-4463.

Gorman, O. T., Bean, W. J., Kawaoka, Y., & Webster, R. G. (1990). Evolution of the nucleoprotein gene of influenza A virus. *Journal of virology*, *64*(4), 1487-1497.

Guilligay, D., Tarendeau, F., Resa-Infante, P., Coloma, R., Crepin, T., Sehr, P., ... & Cusack, S. (2008). The structural basis for cap binding by influenza virus polymerase subunit PB2. *Nature structural & molecular biology*, *15*(5), 500-506.

Hagiwara, K., Kondoh, Y., Ueda, A., Yamada, K., Goto, H., Watanabe, T., ... & Aida, Y. (2010). Discovery of novel antiviral agents directed against the influenza A virus nucleoprotein using photo-cross-linked chemical arrays. *Biochemical and biophysical research communications*, *394*(3), 721-727.

Hai, R., Schmolke, M., Leyva-Grado, V. H., Thangavel, R. R., Margine, I., Jaffe, E. L., ... & Bouvier, N. M. (2013). Influenza A (H7N9) virus gains neuraminidase inhibitor resistance without loss of in vivo virulence or transmissibility. *Nature communications*, *4*.

Hara, K., Schmidt, F. I., Crow, M., & Brownlee, G. G. (2006). Amino acid residues in the N-terminal region of the PA subunit of influenza A virus RNA polymerase play a critical role in protein stability, endonuclease activity, cap binding, and virion RNA promoter binding. *Journal of virology*, *80*(16), 7789-7798.

Hay, A. J., Wolstenholme, A. J., Skehel, J. J., & Smith, M. H. (1985). The molecular basis of the specific anti-influenza action of amantadine. *The EMBO journal*, *4*(11), 3021.

He, X., Zhou, J., Bartlam, M., Zhang, R., Ma, J., Lou, Z., ... & Ge, R. (2008). Crystal structure of the polymerase PAC–PB1N complex from an avian influenza H5N1 virus. *Nature*, *454*(7208), 1123-1126.

Holsinger, L. J., Nichani, D., Pinto, L. H., & Lamb, R. A. (1994). Influenza A virus M2 ion channel protein: a structure-function analysis. *Journal of virology*, *68*(3), 1551-1563.

Honda, A., Ueda, K., Nagata, K., & Ishihama, A. (1988). RNA polymerase of influenza virus: role of NP in RNA chain elongation. *Journal of biochemistry*, *104*(6), 1021-1026.

Hurt, A. C., Selleck, P., Komadina, N., Shaw, R., Brown, L., & Barr, I. G. (2007). Susceptibility of highly pathogenic A (H5N1) avian influenza viruses to the neuraminidase inhibitors and adamantanes. *Antiviral research*, *73*(3), 228-231.

Jagger, B. W., Wise, H. M., Kash, J. C., Walters, K. A., Wills, N. M., Xiao, Y. L., ... & Dalton, R. M. (2012). An overlapping protein-coding region in influenza A virus segment 3 modulates the host response. *Science*, *337*(6091), 199-204.

Jin, Z., Smith, L. K., Rajwanshi, V. K., Kim, B., & Deval, J. (2013). The ambiguous base-pairing and high substrate efficiency of T-705 (favipiravir) ribofuranosyl 5′-triphosphate towards influenza A virus polymerase. *PLoS One*, *8*(7), e68347.

Jing, X., Ma, C., Ohigashi, Y., Oliveira, F. A., Jardetzky, T. S., Pinto, L. H., & Lamb, R. A. (2008). Functional studies indicate amantadine binds to the pore of the influenza A virus M2 proton-selective ion channel. *Proceedings of the National Academy of Sciences*, *105*(31), 10967-10972.

Jorba, N., Coloma, R., & Ortín, J. (2009). Genetic trans-complementation establishes a new model for influenza virus RNA transcription and replication. *PLoS Pathog*, *5*(5), e1000462.

Kao, R. Y., Yang, D., Lau, L. S., Tsui, W. H., Hu, L., Dai, J., ... & Sun, J. (2010). Identification of influenza A nucleoprotein as an antiviral target. *Nature biotechnology*, *28*(6), 600-605.

Kawaguchi, A., Momose, F., & Nagata, K. (2011). Replication-coupled and host factor-mediated encapsidation of the influenza virus genome by viral nucleoprotein. *Journal of virology*, *85*(13), 6197-6204.

Kiso, M., Mitamura, K., Sakai-Tagawa, Y., Shiraishi, K., Kawakami, C., Kimura, K., ... & Kawaoka, Y. (2004). Resistant influenza A viruses in children treated with oseltamivir: descriptive study. *The Lancet*, *364*(9436), 759-765.

Kiso, M., Takahashi, K., Sakai-Tagawa, Y., Shinya, K., Sakabe, S., Le, Q. M., ... & Kawaoka, Y. (2010). T-705 (favipiravir) activity against lethal H5N1 influenza A viruses. *Proceedings of the National Academy of Sciences*, *107*(2), 882-887.

Kuzuhara, T., Kise, D., Yoshida, H., Horita, T., Murazaki, Y., Nishimura, A., ... & Tsuge, H. (2009). Structural basis of the influenza A virus RNA polymerase PB2 RNA-binding domain containing the pathogenicity-determinant lysine 627 residue. *Journal of Biological Chemistry*, *284*(11), 6855-6860.

Labadie, K., Afonso, E. D. S., Rameix-Welti, M. A., Van Der Werf, S., & Naffakh, N. (2007). Host-range determinants on the PB2 protein of influenza A viruses control the interaction between the viral polymerase and nucleoprotein in human cells. *Virology*, *362*(2), 271-282.

Lejal, N., Tarus, B., Bouguyon, E., Chenavas, S., Bertho, N., Delmas, B., ... & Slama-Schwok, A. (2013). Structure-based discovery of the novel antiviral properties of naproxen against the nucleoprotein of influenza A virus. *Antimicrobial agents and chemotherapy*, *57*(5), 2231-2242.

Li, L., Chang, S. H., Xiang, J. F., Li, Q., Liang, H. H., Tang, Y. L., & Liu, Y. F. (2012). NMR identification of anti-influenza lead compound targeting at PA C subunit of H5N1 polymerase. *Chinese Chemical Letters*, *23*(1), 89-92.

Li, M. L., Rao, P., & Krug, R. M. (2001). The active sites of the influenza cap-dependent endonuclease are on different polymerase subunits. *The EMBO journal*, *20*(8), 2078-2086.

Li, Z., Watanabe, T., Hatta, M., Watanabe, S., Nanbo, A., Ozawa, M., ... & Kawaoka, Y. (2009). Mutational analysis of conserved amino acids in the influenza A virus nucleoprotein. *Journal of virology*, *83*(9), 4153-4162.

Lin, L., Li, Y., Pyo, H. M., Lu, X., Raman, S. N. T., Liu, Q., ... & Zhou, Y. (2012). Identification of RNA helicase A as a cellular factor that interacts with influenza A virus NS1 protein and its role in the virus life cycle. *Journal of virology*, *86*(4), 1942-1954.

Maier, H. J., Kashiwagi, T., Hara, K., & Brownlee, G. G. (2008). Differential role of the influenza A virus polymerase PA subunit for vRNA and cRNA promoter binding. *Virology*, *370*(1), 194-204.

Marklund, J. K., Ye, Q., Dong, J., Tao, Y. J., & Krug, R. M. (2012). Sequence in the influenza A virus nucleoprotein required for viral polymerase binding and RNA synthesis. *Journal of virology*, *86*(13), 7292-7297.

Massin, P., Van der Werf, S., & Naffakh, N. (2001). Residue 627 of PB2 is a determinant of cold sensitivity in RNA replication of avian influenza viruses. *Journal of virology*, *75*(11), 5398-5404.

Meindl, P., Bodo, G., Palese, P., Schulman, J., & Tuppy, H. (1974). Inhibition of neuraminidase activity by derivatives of 2-deoxy-2, 3-dehydro-N-acetylneuraminic acid. *Virology*, *58*(2), 457-463.

Menéndez-Arias, L., Álvarez, M., & Pacheco, B. (2014). Nucleoside/nucleotide analog inhibitors of hepatitis B virus polymerase: mechanism of action and resistance. *Current opinion in virology*, *8*, 1-9.

Momose, F., Basler, C. F., O'Neill, R. E., Iwamatsu, A., Palese, P., & Nagata, K. (2001). Cellular splicing factor RAF-2p48/NPI-5/BAT1/UAP56 interacts with the influenza virus nucleoprotein and enhances viral RNA synthesis. *Journal of Virology*, *75*(4), 1899-1908.

Muramoto, Y., Noda, T., Kawakami, E., Akkina, R., & Kawaoka, Y. (2012). Identification of novel influenza A virus proteins translated from PA mRNA. *Journal of virology*, *87*(5), 2455-2462.

Muratore, G., Goracci, L., Mercorelli, B., Foeglein, Á., Digard, P., Cruciani, G., ... & Loregian, A. (2012). Small molecule inhibitors of influenza A and B

viruses that act by disrupting subunit interactions of the viral polymerase. *Proceedings of the National Academy of Sciences*, *109*(16), 6247-6252.

Neumann, G., Noda, T., & Kawaoka, Y. (2009). Emergence and pandemic potential of swine-origin H1N1 influenza virus. *Nature*, *459*(7249), 931-939.

Newcomb, L. L., Kuo, R. L., Ye, Q., Jiang, Y., Tao, Y. J., & Krug, R. M. (2009). Interaction of the influenza a virus nucleocapsid protein with the viral RNA polymerase potentiates unprimed viral RNA replication. *Journal of virology*, *83*(1), 29-36.

Ng, A. K. L., Chan, W. H., Choi, S. T., Lam, M. K. H., Lau, K. F., Chan, P. K. S., ... & Shaw, P. C. (2012). Influenza polymerase activity correlates with the strength of interaction between nucleoprotein and PB2 through the host-specific residue K/E627. *PLoS One*, *7*(5), e36415.

Obayashi, E., Yoshida, H., Kawai, F., Shibayama, N., Kawaguchi, A., Nagata, K., ... & Park, S. Y. (2008). The structural basis for an essential subunit interaction in influenza virus RNA polymerase. *Nature*, *454*(7208), 1127-1131.

Oestereich, L., Lüdtke, A., Wurr, S., Rieger, T., Muñoz-Fontela, C., & Günther, S. (2014). Successful treatment of advanced Ebola virus infection with T-705 (favipiravir) in a small animal model. *Antiviral research*, *105*, 17-21.

Palese, P., Schulman, J. L., Bodo, G., & Meindl, P. (1974). Inhibition of influenza and parainfluenza virus replication in tissue culture by 2-deoxy-2, 3-dehydro-N-trifluoroacetylneuraminic acid (FANA). *Virology*, *59*(2), 490-498.

Pautus, S., Sehr, P., Lewis, J., Fortuné, A., Wolkerstorfer, A., Szolar, O., ... & Cusack, S. (2013). New 7-methylguanine derivatives targeting the influenza polymerase PB2 cap-binding domain. *J. Med. Chem*, *56*(21), 8915-8930.

Pérez, D. R., & Donis, R. O. (1995). A 48-amino-acid region of influenza A virus PB1 protein is sufficient for complex formation with PA. *Journal of virology* 69(11), 6932-6939.

Pérez, D. R., & Donis, R. O. (2001). Functional analysis of PA binding by influenza a virus PB1: effects on polymerase activity and viral infectivity. *Journal of virology*, *75*(17), 8127-8136.

Perry, N. B., Blunt, J. W., Munro, M. H., & Pannell, L. K. (1988). Mycalamide A, an antiviral compound from a New Zealand sponge of the genus Mycale. *Journal of the American Chemical Society*, *110*(14), 4850-4851.

Pinto, L. H., Holsinger, L. J., & Lamb, R. A. (1992). Influenza virus M 2 protein has ion channel activity. *Cell*, *69*(3), 517-528.

Pizzorno, A., Abed, Y., Bouhy, X., Beaulieu, É., Mallett, C., Russell, R., & Boivin, G. (2012). Impact of mutations at residue I223 of the neuraminidase protein on the resistance profile, replication level, and virulence of the 2009 pandemic influenza virus. *Antimicrobial agents and chemotherapy*, *56*(3), 1208-1214.

Plotch, S. J., Bouloy, M., Ulmanen, I., & Krug, R. M. (1981). A unique cap (m7GpppXm)-dependent influenza virion endonuclease cleaves capped RNAs to generate the primers that initiate viral RNA transcription. *Cell*, *23*(3), 847-858.

Poon, L. L., Pritlove, D. C., Fodor, E., & Brownlee, G. G. (1999). Direct evidence that the poly (A) tail of influenza A virus mRNA is synthesized by reiterative copying of a U track in the virion RNA template. *Journal of virology*, *73*(4), 3473-3476.

Portela, A., & Digard, P. (2002). The influenza virus nucleoprotein: a multifunctional RNA-binding protein pivotal to virus replication. *Journal of general virology*, *83*(4), 723-734.

Rameix-Welti, M. A., Tomoiu, A., Afonso, E. D. S., Van Der Werf, S., & Naffakh, N. (2009). Avian influenza A virus polymerase association with nucleoprotein, but not polymerase assembly, is impaired in human cells during the course of infection. *Journal of virology*, *83*(3), 1320-1331.

Reid, A. H., & Taubenberger, J. K. (2003). The origin of the 1918 pandemic influenza virus: a continuing enigma. *Journal of General Virology*, *84*(9), 2285-2292.

Sanchez, A., Guerrero-Juarez, C. F., Ramirez, J., & Newcomb, L. L. (2014). Nuclear localized Influenza nucleoprotein N-terminal deletion mutant is deficient in functional vRNP formation. *Virology journal*, *11*(1), 1.

Shapiro, G. I., & Krug, R. M. (1988). Influenza virus RNA replication in vitro: synthesis of viral template RNAs and virion RNAs in the absence of an added primer. *Journal of virology*, *62*(7), 2285-2290.

Shen, Y. F., Chen, Y. H., Chu, S. Y., Lin, M. I., Hsu, H. T., Wu, P. Y., ... & Hsu, P. H. (2011). E339… R416 salt bridge of nucleoprotein as a feasible target

for influenza virus inhibitors. *Proceedings of the National Academy of Sciences*, *108*(40), 16515-16520.

Shinya, K., Hamm, S., Hatta, M., Ito, H., Ito, T., & Kawaoka, Y. (2004). PB2 amino acid at position 627 affects replicative efficiency, but not cell tropism, of Hong Kong H5N1 influenza A viruses in mice. *Virology*, *320*(2), 258-266.

Shoji, M., Takahashi, E., Hatakeyama, D., Iwai, Y., Morita, Y., Shirayama, R., ... & Okutani, T. (2013). Anti-influenza Activity of C 60 Fullerene Derivatives. *PloS one*, *8*(6), e66337.

Sleeman, K., Mishin, V. P., Deyde, V. M., Furuta, Y., Klimov, A. I., & Gubareva, L. V. (2010). In vitro antiviral activity of favipiravir (T-705) against drug-resistant influenza and 2009 A (H1N1) viruses. *Antimicrobial agents and chemotherapy*, *54*(6), 2517-2524.

Su, G. H., Sohn, T. A., Ryu, B., & Kern, S. E. (2000). A novel histone deacetylase inhibitor identified by high-throughput transcriptional screening of a compound library. *Cancer research*, *60*(12), 3137-3142.

Subbarao, E. K., & Murphy, B. R. (1993). A single amino acid in the PB2 gene of influenza A virus is a determinant of host range. *Journal of virology*, *67*(4), 1761-1764.

Sugiyama, K., Obayashi, E., Kawaguchi, A., Suzuki, Y., Tame, J. R., Nagata, K., & Park, S. Y. (2009). Structural insight into the essential PB1–PB2 subunit contact of the influenza virus RNA polymerase. *The EMBO journal*, *28*(12), 1803-1811.

Takahashi, K., Smee, D. F., Shiraki, K., Kawaoka, Y., & Furuta, Y. (2011). Pharmacological effects of favipiravir, an anti-influenza viral drug. *J Med Pharm Sci*, *66*, 429-441.

Tang, J. W., Ngai, K. L., Wong, J. C., Lam, W. Y., & Chan, P. K. (2008). Emergence of adamantane‐resistant influenza A (H3N2) viruses in Hong Kong between 1997 and 2006. *Journal of medical virology*, *80*(5), 895-901.

Tarendeau, F., Crepin, T., Guilligay, D., Ruigrok, R. W., Cusack, S., & Hart, D. J. (2008). Host determinant residue lysine 627 lies on the surface of a discrete, folded domain of influenza virus polymerase PB2 subunit. *PLoS Pathog*, *4*(8), e1000136.

van der Vries, E., Kroeze, E. J. V., Stittelaar, K. J., Linster, M., Van der Linden, A., Schrauwen, E. J., ... & Osterhaus, A. D. (2011). Multidrug resistant 2009 A/H1N1 influenza clinical isolate with a neuraminidase I223R mutation retains its virulence and transmissibility in ferrets. *PLoS Pathog*, *7*(9), e1002276.

Wang, P., Palese, P., & O'Neill, R. E. (1997). The NPI-1/NPI-3 (karyopherin alpha) binding site on the influenza a virus nucleoprotein NP is a nonconventional nuclear localization signal. *Journal of virology*, *71*(3), 1850-1856.

WHO. http://www.who.int/influenza/human_animal_interface/avian_influenza/h5n1_research/faqs/en/.

Wise, H. M., Foeglein, A., Sun, J., Dalton, R. M., Patel, S., Howard, W., ... & Digard, P. (2009). A complicated message: Identification of a novel PB1-

related protein translated from influenza A virus segment 2 mRNA. *Journal of virology*, *83*(16), 8021-8031.

Wisskirchen, C., Ludersdorfer, T. H., Müller, D. A., Moritz, E., & Pavlovic, J. (2011). The cellular RNA helicase UAP56 is required for prevention of double-stranded RNA formation during influenza A virus infection. *Journal of virology*, *85*(17), 8646-8655.

Wunderlich, K., Mayer, D., Ranadheera, C., Holler, A. S., Mänz, B., Martin, A., ... & Schwemmle, M. (2009). Identification of a PA-binding peptide with inhibitory activity against influenza A and B virus replication. *PLoS One*, *4*(10), e7517.

Ye, Q., Krug, R. M., & Tao, Y. J. (2006). The mechanism by which influenza A virus nucleoprotein forms oligomers and binds RNA. *Nature*, *444*(7122), 1078-1082.

Ye, Q., Guu, T. S., Mata, D. A., Kuo, R. L., Smith, B., Krug, R. M., & Tao, Y. J. (2013). Biochemical and structural evidence in support of a coherent model for the formation of the double-helical influenza A virus ribonucleoprotein. *MBio*, *4*(1), e00467-12.

Yuan, P., Bartlam, M., Lou, Z., Chen, S., Zhou, J., He, X., ... & Fodor, E. (2009). Crystal structure of an avian influenza polymerase PAN reveals an endonuclease active site. *Nature*, *458*(7240), 909-913.

Zhao, C., Lou, Z., Guo, Y., Ma, M., Chen, Y., Liang, S., ... & Bartlam, M. (2009). Nucleoside monophosphate complex structures of the endonuclease

domain from the influenza virus polymerase PA subunit reveal the substrate binding site inside the catalytic center. *Journal of virology*, *83*(18), 9024-9030.